Optimal influent N-to-P ratio for stable microalgal cultivation in water treatment and nutrient recovery

Dorottya S. Wágner[*,a,b], Clarissa Cazzaniga[a], Michael Steidl[a], Arnaud Dechesne[a], Borja Valverde-Pérez[a], Benedek Gy. Plósz[*,a,c]

[a] *Department of Environmental Engineering, Technical University of Denmark, Miljøvej, Building 115, 2800 Kgs. Lyngby, Denmark*

[c] *Department of Chemical Engineering, University of Bath, Claverton Down, Bath BA2 7AY, UK*

**Corresponding authors: dsw@bio.aau.dk; bgp24@bath.ac.uk*

Abstract

Species specific nitrogen-to-phosphorus molar ratio (NPR) has been suggested for green microalgae. Algae can store nitrogen and phosphorus, suggesting that the optimum feed concentration dynamically changes as function of the nutrient storage. We assessed the effect of varying influent NPR on microalgal cultivation in terms of microbial community stability, effluent quality and biokinetics. Mixed green microalgae (*Chlorella sorokiniana* and *Scenedesmus sp.*) and a monoculture of *Chlorella sp.* were cultivated in continuous laboratory-scale reactors treating used water. An innovative image analysis tool, developed in this study, was used to track microbial community changes. Diatoms proliferated as influent NPR decreased, and were outcompeted once cultivation conditions were restored to the optimal NPR range. Low NPR operation resulted in decrease in phosphorus removal, biomass concentration and effluent nitrogen concentration. ASM-A kinetic model simulation results agreed well with operational data in the absence of diatoms. The failure to predict operational data in the presence of diatoms suggest differences in microbial activity that can significantly influence nutrient recovery in photobioreactors (PBR). No contamination occurred

[b] *Current address: Department of Chemistry and Bioscience, Aalborg University, Fredrik Bajers Vej 7H, 9220 Aalborg, Denmark*

during *Chlorella sp.* monoculture cultivation with varying NPRs. Low NPR operation resulted in decrease in biomass concentration, effluent nitrogen concentration and nitrogen quota. The ASM-A model was calibrated for the monoculture and the simulations could predict the experimental data in continuous operation using a single parameter subset, suggesting stable biokinetics under the different NPR conditions. Results show that controlling the influent NPR is effective to maintain the algal community composition in PBR, thereby ensuring effective nutrients conversion.

Keywords

nitrogen-to-phosphorus ratio; algal cultivation; algal diversity control in photobioreactors; process modelling; resource recovery; ecological interactions in photobioreactors

1. Introduction

Microalgal cultivation on used water resources has high potential for resource recovery. Cultivation is mostly done in open systems, where the potential of contamination is high. Used water is a potential source of energy, nutrients (nitrogen and phosphorus) and fresh water. However, conventional used water treatment focuses on the destruction of organic and inorganic constituents (Batstone et al., 2015) through energy-intensive processes. Current research aims to develop new technologies to reduce energy requirements (Gao et al., 2014) and facilitate resource recovery (Verstraete and Vlaeminck, 2011). Microalgae cultivation has been proposed as a means to recover resources from used water (Cai et al., 2013; Gardner-Dale et al., 2017; Matassa et al., 2015; Mehta et al., 2015). Combining microalgae cultivation with used water resource recovery can result in production of biomass suitable for biofuel production (Geiss et al., 2015; Mata et al., 2010; Wágner et al., 2016a). Moreover, microalgal biomass can be used as natural slow-leaching fertiliser, thereby recycling nutrients present in the used water (Coppens et al., 2016; Solovchenko et al., 2016), or as an alternative source of protein (Matassa et al., 2015; Rasouli et al., 2018).

Many reactor configurations and cultivation methods have been proposed to grow microalgae on used water resources. Most of these systems consider open cultivation e.g., (Alcántara et al., 2015; Béchet et al., 2016; Sforza et al., 2014; Sutherland et al., 2014; Van Den Hende et al., 2014). Variation in the nutrient composition of influent water is reported to affect nutrient removal and thus effluent quality (Arbib et al., 2013). Therefore, using different wastewater streams for microalgae cultivation might compromise nutrient removal (Wang et al., 2010). Furthermore, nutrient loads and balances affect algal composition (De Francisci et al., 2018). When nitrogen or phosphorus are limiting, algae store inorganic carbon as starch and lipids, thus promoting algal biomass into an appealing feedstock for biofuel production (Ikaran et al., 2015; Mayers et al., 2014). Under nutrient limiting conditions, algae also shift pigmentation, usually producing more carotenoids, such as lutein, which are valuable antioxidants for food and feed industries (Safafar et al., 2015; Wágner et al., 2018). On the contrary, if nutrients are fed in excess, algae can store large quantities of phosphorus, e.g., as polyphosphates (Powell et al., 2011), and nitrogen, e.g., as protein (Gardner-Dale et al., 2017). Therefore, for the particular goal of water resource recovery, the effect of dynamic nitrogen-to-phosphorus molar ratio (NPR) on algal cultivation needs to be better understood.

A two-stage bacterial-algal cultivation for nutrient removal from used water was proposed by Valverde-Pérez et al. (2015), whereby an enhanced biological phosphorus recovery and removal (EBP2R) process provides optimal cultivation media for green microalgal growth. The combined EBP2R and algal photobioreactor (PBR) is referred to as TRENS system (Fang et al., 2016). The system produces an algal suspension where nutrients are stored in the algal biomass rather than present in the bulk liquid, which can be used for fertigation. The TRENS system offers the flexibility of cultivating different microalgal species under optimal conditions from a given used water source. In order to keep a stable NPR for algal cultivation, Valverde-Pérez et al. (2016a) proposed a control design structure for EBP2R systems. The study found that, under highly dynamic conditions, the

effluent NPR presented some variability around the optimal ratio. Therefore, understanding the nutrients requirements and the optimal NPR of microalgal cultivation in dynamic used water systems is essential.

As used water contains diverse microorganisms, such as algae and protozoa (Henze et al., 2008), there is high risk of contamination, especially in open reactors, which may compromise algal cultivation (Montemezzani et al., 2015). Thus, robust microalgal species or mixed microalgal consortia are preferred for long term reactor operation (Novoveská et al., 2016). Lynch et al. (2015) suggest the use of native species, which would outperform other microorganisms. Moreover, species that can be cultivated in selective environments, such as high salinity or alkalinity, would reduce the risk of contamination in such systems. Furthermore, promoting microalgal growth by optimized cultivation (e.g. sufficient light availability, mixing, NPR and inorganic carbon source) can help maintain the species composition (Borowitzka and Moheimani, 2013).

The optimal NPR of algae has been an interest since the 1950s, when Redfield (1958) found that the optimal NPR in marine phytoplankton was 16 mol-N/mol-P. Since then, many researchers have suggested that the optimal NPR in microalgae is species specific (Anbalagan et al., 2016; Beuckels et al., 2015; Rhee and Gotham, 1980; Whitton et al., 2016) and may vary depending on cultivation conditions, indicating microalgae adaptability to the culture conditions (Arbib et al., 2013; Beuckels et al., 2015; Boelee et al., 2011; Dickinson et al., 2013; Gardner-Dale et al., 2017; Geider and La Roche, 2002; Liu and Vyverman, 2015; Marcilhac et al., 2015; Rhee, 1978).

Therefore, the objectives of this study are: (i) to assess the effect of influent NPR on culture composition in a mixed consortium and a monoculture during continuous cultivation; (ii) to assess the effect of algal culture composition on nutrient recovery; (iii) propose PBR operational strategies to maintain high nutrient recovery efficiency in open PBR processes.

93 # 2. Materials and methods

94 ## 2.1. Microalgae and culture media

95 *2.1.1. Continuous microalgal cultivation using a mixed green microalgal consortium*

96 A mixed green microalgal consortium, isolated from a natural pond in contact with wastewater,
97 mainly consisting of *Chlorella sorokiniana* and *Scenedesmus sp.* (Supporting Information (SI), Fig.
98 S1) was used in this study (for further information on the culture characterization, the reader is
99 referred to Wágner et al. (2016b)). The consortium was cultivated for 21 days on used water treated
100 by a laboratory scale low-SRT enhanced biological phosphorus removal system (EBPR) operated as
101 a sequencing batch reactor (SBR) at 3 days SRT. The treated used water was not sterilized prior to
102 feeding the mixed algal consortium. The EBPR was fed with used water collected at Mølleåværket
103 WWTP (Kgs. Lyngby, Denmark). Details on the operation of the EBPR system can be found
104 elsewhere (Valverde-Pérez et al., 2016b).

105 *2.1.2. Continuous microalgal cultivation using Chlorella sp.*

106 Two reactors in continuous operation were run for 85 days with *Chlorella sp.* (identified based on
107 microscopy, Fig. S1a, SI). The culture originated from the mixed consortium described in the
108 previous section. However, *Scenedesmus sp.* was outcompeted before the start of this experiment.
109 The culture was fed with treated used water collected from a laboratory scale continuous EBPR
110 system operated at 16 days solids retention time, SRT (Fig. S2, SI). More details on the operation of
111 the continuous EBPR can be found in the Supporting Information (page 9, SI, (Valverde-Pérez,
112 2015)). The influent used water fed to the EBPR was taken from Mølleåværket WWTP (Kgs. Lyngby,
113 Denmark).

114 ## 2.2. Microalgal cultivation in 1.4 L continuous PBR

115 2.2.1 *Continuous reactor operation using the mixed green microalgal consortium*

116 A cylindrical glass PBR with a working volume of 1.4 L was operated in the laboratory. The SRT
117 was the same as the hydraulic residence time (HRT) in the system and it was kept at 2 days. Constant
118 aeration at a flow rate of 30 L/h was used to mix and keep the microalgae in suspension. CO_2 was
119 mixed to the air in a ratio 8-12% to maintain the pH in the 6.5-7.2 range. The reactor was kept at
120 ambient temperature (23-26 °C). Based on previous experience with the mixed culture (Wágner et
121 al., 2016b), light in the visible spectrum was continuously supplied from the top of the reactor at an
122 average intensity of 800 ± 200 µmol photons m^{-2} s^{-1} with a custom-built lamp, with a metal-halide
123 bulb (OSRAM©, Germany). The reactors were covered with a black cloth around the wall, to avoid
124 light entering from the side and to mitigate the daily light intensity changes that would occur in a
125 laboratory. The treated used water, serving as the influent to the PBR, was kept at approximately 5
126 ºC. The pH was adjusted to 6.5-7 (with HCl addition) to avoid phosphorus precipitation in the feed.
127 The NPR of the influent to the PBR was varied during the cultivation. The NPR in this study is
128 expressed as nitrogen-to-phosphorus molar ratio. During the first 6.5 days the influent NPR was kept
129 at 17.6±1.6, selected based on previous experience with the mixed culture (Wágner et al., 2016b).
130 Then, the NPR was lowered to 5.2 until day 10.5 and finally back to 16.5±0.1 until the end of the
131 operation. The influent phosphorus concentration was kept constant at 6±0.7 mg-P/L by adding
132 KH_2PO_4 (Sigma Aldrich), whilst the ammonium concentration was adjusted to reach the required
133 NPR by adding NH_4HCO_3 (Sigma Aldrich) as nitrogen source.

134 *2.2.2 Continuous reactor operation using Chlorella sp.*

135 Two 1.4 L glass cylindrical PBRs were used as described in the previous section. The SRT and HRT
136 in the system were kept at 3.5 days. Constant aeration mixed with CO_2 in 30-40 % ratio was used at
137 a flow rate of 20 L/h to adjust the pH in the range of 6.5-7.5 and mix the suspension. Light was

supplied from the top of the reactors continuously with a custom-built lamp, providing in average 1262 ± 314 μmol photons m^{-2} s^{-1}, with a metal-halide light bulb (OSRAM©, Germany). The reactors were covered with a black cloth around the wall, to avoid light entering from the side of the reactor (Fig. S3a, SI) and to mitigate the daily light intensity changes that would occur in a laboratory. The cultivation was done at room temperature (approximately 21 ºC) until a sudden increase in ambient temperature due to the summer weather conditions (this period, from day 45 to day 58 is not discussed in this study). The reactor temperature was then controlled with a cooling system, whereby cold tap water was circulated around the PBR surface to lower the temperature inside the reactor to approximately to 21 ºC (Fig. S3b, SI). The treated used water, which served as the influent to the PBR, was kept at approximately 5 ºC. The pH was adjusted to 6.5-7 (with HCl addition) to avoid phosphorus precipitation in the feed. Two identical reactors were operated in parallel. One reactor was chosen as a reference (Reactor 1 (R1)) and was operated at constant influent NPR of 17.3±2. In a second reactor (Reactor 2 (R2)) the influent to the PBR was varied. During the first 21 days the influent NPR was kept at 16.8±2, then lowered to 10.3±0.33 until day 37, and finally back to 17.9±0.5 until day 45. The NPR in the second reactor was kept at 17.3±3 until day 71, when it was increased to 25.8±1.7 until day 85, the end of the reactor operation. The nitrogen and ortho-phosphate concentrations were adjusted to reach the required NPR by adding $NaNO_3$ (Sigma Aldrich) as nitrogen and KH_2PO_4 (Sigma Aldrich) as phosphorus source. The phosphorus concentration was kept constant at 3.9±0.33 mg-P/L and nitrogen was varied to reach the required NPR.

2.3. Image analysis for community composition description

The culture in each experiment was monitored using an innovative image analysis method developed during this study. One drop of suspension was taken with a disposable plastic pipette and the droplet was covered with a cover slip. Bright field imaging was done using a Motic AE31 microscope (Hong Kong) with a magnification of 20x. For image analysis, the software Image pro plus 7 3D suite (Media

Cybernetics, MD, USA) was used to automate the identification and quantification of the different types of algae based on their morphology. The different types of green microalgae were distinguished according to their morphology: i.e. *Chlorella sp.* (round and small individual cells, Fig. S1a, SI) and *Scenedesmus sp.* (elongated cells forming two-to-four-cell colonies, Fig. S1b, SI). The diatoms that appeared during cultivation could also be identified based on their morphology (elongated cells, larger than the other two species, Fig. S5a, SI). To distinguish between the genera, morphological descriptors (area, diameter, the aspect ratio, which is the ratio between the longest and shortest diameter and axis, which describes the long narrow algae) of each type were automatically acquired using the image analysis software. The morphological parameters (Table S2, SI) were observed to be culture condition specific. Therefore, it is suggested to calibrate the morphological parameters every time a new consortium is studied. The required number of images for the analysis of estimating the distribution of different species was tested on both the mixed culture (containing *Chlorella sp.* and *Scenedesmus sp.*) and the monoculture (containing *Chlorella sp.*) by taking up to 50 images and assessing the cell count and the cell area based on the number of images. The required number of images for the mixed culture was found to be 20, whilst for the monoculture it was 10 (Fig. S4, SI).

2.4. Batch experiments for model calibration

Three batch experiments were set up using a glass cylinder with a working volume of 1.2 L. Continuous lighting was provided by one custom-built lamp with a metal-halide light bulb (OSRAM©, Germany) from the top of the reactor with an average light intensity of 1000 ± 121 µmol photons m^{-2} s^{-1}. CO_2 enriched airflow was supplied from the bottom of the reactor at 20 L/h and at 30-40 % CO_2 to guarantee full mixing and to keep pH between 6.5 and 7.5. The batch was prepared using 1 L of effluent from the laboratory scale EBPR system and 200 ml of effluent from the second continuous PBR containing *Chlorella sp*. The inoculum for the first batch was taken on day 21, when the culture was adjusted to an NPR of 16.8±2. The second batch was inoculated with algae taken on

day 37, when the culture was adjusted to an NPR of 10.3±0.3. Finally, the inoculum for batch 3 was taken on day 79, when the culture was cultivated at 25.8±1.7 NPR. The experiments were run with an initial NPR of 17. The required nitrogen and phosphorus concentrations were obtained by spiking $NaNO_3$ and KH_2PO_4 solutions. The initial conditions of the three experiments can be found in Table S1, SI.

2.5. Model based assessment, model calibration and statistical analysis

The ASM-A process model, developed in a previous study (Wágner et al., 2016b), was used for the simulations and parameter estimation. ASM-A, implemented in Matlab (The MathWorks, Natick, Massachusetts, USA) can predict the uptake and storage of nitrogen and phosphorus as well as microalgal growth and decay under photoautotrophic and heterotrophic conditions. Default parameters were used for the mixed culture and model was recalibrated when assessing the monoculture performance. Parameter estimation was carried out based on the global optimisation method for parameter estimation, Latin Hypercube Sampled priors for Simplex (LHSS) (Wágner et al., 2016b). 500 simulations were found sufficient to reach convergence for parameter estimation. Values for parameters not estimated in this study were taken from the original ASM-A calibration. The average light intensity in the reactor was calculated based on integration of the Lambert-Beer law. However, in this study we used a time variable average light intensity, by calculating it for each time step and updating it during the model simulations. The incident light intensity varied during the batch experiments, due to the decrease of the height of the suspension in the reactor resulting from the daily sampling. Thus, the incident light intensity was updated during the simulations (see level of complexity 2 for light modelling in (Wágner et al., 2018)). The Janus coefficient was calculated for model evaluation (Sin et al., 2008). The model parameter estimates are validated when the Janus coefficient approaches 1.

2.6. Analytical methods and calculations

Biomass in the continuous and batch reactors was analysed by measuring the total suspended solids (TSS) using glass fibre filter (Advantec©, USA) with a pore size of 0.6 μm (APHA et al., 1999). Total COD, total nitrogen and phosphorus measurements in the suspension were done using commercial test kits (Hach-Lange©, CO, USA). Following sample filtration (0.2 μm filter), ammonium, nitrate, nitrite and phosphate concentrations were measured using test kits supplied by Merck© (NJ, USA) and soluble COD was measured using Hach-Lange© test kits (CO, USA). The COD of the microalgal biomass was calculated by the difference of the total and soluble COD. The TSS to COD conversion factor was estimated to be in average 0.9 (calculated as described in SI). The internal cell quota of nitrogen was calculated based on the difference of total nitrogen in the algal suspension (algae+medium) and total soluble nitrogen in the filtrate (soluble organic N, NH_4^+, NO_2^- and NO_3^-). The internal cell quota of phosphorus was obtained by the difference of total phosphorus in the algal suspension and soluble phosphate in the filtrate. Incoming light intensity and pH were monitored using LI-1400 Data Logger with LI-193 Spherical Underwater Quantum Sensor (LI-COR, USA) and Multi 3430 Digital pH meter for pH-Electrode Sentix 940 sensor (WTW, Germany), respectively. The pigment content of the biomass was measured as described in Wágner et al. (Wágner et al., 2018). Chlorophyll a and b as well as some carotenoids (lutein, β-carotene, violaxanthin) were targeted during the analysis.

Protein content was calculated by multiplying the nitrogen quota by a nitrogen-to-protein factor as suggested by Gardner-Dale et al. (Gardner-Dale et al., 2017). Nitrogen-to-protein conversion factor value was taken from Templeton and Laurens (Templeton and Laurens, 2015). For *Chlorella sp.* it is reported to be 5.04 g protein/g N.

3. Results and discussion

3.1. Impact of varying nutrient availability on microalgal diversity

3.1.1. Mixed culture dynamics

The image analysis tool was used to monitor the culture composition in the mixed microalgal consortium. At the beginning of the cultivation the mixed microalgal consortium contained mostly *Scenedesmus sp.*, about 83% of the total cell count (Fig. 1). *Chlorella sp.* were present at 9% along with some other species belonging mainly to phylum *Chlorophyta* and some smaller ciliates at 8%. The composition did not change in the first period of the cultivation, when the NPR was 17.6±1.6. When the influent NPR was lowered to 5.2, there was a sudden appearance of diatoms identified as *Nitzschia sp.* based on microscopic observation (Fig. S5a, SI). These diatoms were seeded from the influent water to the PBR (based on microscopic observations) that probably originated from the WWTP and proliferated under the altered cultivation conditions. Indeed, diatoms have been reported as indigenous algae species in sewage streams in Scandinavia (Krustok et al., 2015). Many diatoms have lower NPR compared to the mixed culture used in this study (Dang et al., 2018), so lower NPR may have selected for their growth. Furthermore, diatoms are able to grow in waters with very limited nitrogen availability. Indeed, the affinity coefficients reported for these microalgae are considerably lower compared to those reported for the mixed culture used in this study (ammonia affinity coefficients for diatoms are in the order of $1\text{-}10^{-3}$ mg-N/L, Fan et al., 2003, compared to 4-10 mg-N/L for our mixed culture, Wágner et al., 2016b), which make them efficient k-strategists. Alternatively, diatoms build synergies with cyanobacteria in low nutrient environments, whereby cyanobacteria fix atmospheric nitrogen and make it bioavailable for diatoms (Foster et al., 2011). Considering these aspects, when decreasing the ammonium in the influent to decrease the NPR, diatoms were still able to grow in the PBR, while the mixed culture's growth was limited. When NPR

was above 16, nitrogen was not a limiting growth factor, thus promoting fast growing green microalgae (e.g., *Chlorella sp.*, which are r-strategists; Galès et al., 2019). The amount of diatoms increased to up to 8% of total cell count by day 10. Their relative abundance was much larger when accounting for the cell area (up to 34%), due to their 3-5 times higher cell size relative to *Chlorella sp.* and *Scenedesmus sp.* The cell area is relevant as it can be related to the TSS of the biomass (Fig. S6, SI), and thus it can allow the approximation of the mass fraction of the different species. Thus, although the cell count of diatoms was low compared to the other species, diatoms constituted a significant fraction of the biomass concentration. Moreover, the number and the size of ciliates increased in the reactor (Fig. S5b, SI), yielding a significant increase of the relative cell area of other non-classified species (66%, Fig. 1). However, ciliates were quickly washed out at day 10 (Fig. 1). Diatoms contain on several metabolites that can have a detrimental effect on the reproduction of ciliates (Miralto et al., 1999). Thus, the proliferation of diatoms in the PBR served to control ciliates population, which fed on them, and eventually led to lower numbers of these predators once the NPR was restored. The presence of ciliates and other grazers act as selective factor promoting the co-existence of *Chlorella sp.* and *Scenedesmus sp.*, as the second is more resilient to predators despite its comparably lower growth rates (Galès et al., 2019). On day 8, the fraction of *Chlorella sp.* started to increase while *Scenedesmus sp.* decreased. Nevertheless, by day 10, their cell count was reduced, possibly due to the presence of grazers that prefer *Chlorella* over *Scenedesmus sp.* due to their smaller size (Borowitzka and Moheimani, n.d.). After the NPR was set back to 16.5±0.1, the diatoms were outcompeted from the system, suggesting that the cultivation conditions were more optimal for *Chlorella* and *Scenedesmus sp.* Interestingly, the relative ratio of *Chlorella* and *Scenedesmus sp.* had shifted from day 11 to 21, reaching 77% of *Chlorella sp.* of the total cell count at day 21 (Fig. 1). Alcántara et al. (Alcántara et al., 2015) similarly observed that *Scenedesmus sp.* were initially more abundant, whilst by the end of the cultivation period *Chlorella sp*. proliferated. Thus, it is

hypothesised that the cultivation conditions are more optimal for *Chlorella sp.* than *Scenedesmus sp.* in our case, also supported by Beuckels et al. (Beuckels et al., 2015), who found that *Chlorella sp.* is capable of accumulating more nitrogen than *Scenedesmus sp*. This contradicts with other studies which showed that *Scenedesmus sp.* prefer larger NPR than *Chlorella sp.* when phosphorus concentration is varied (Marcilhac et al., 2015).

<Figure 1>

3.1.2. Monoculture dynamics

A monoculture of *Chlorella sp.* was cultivated in continuous reactor operation using effluent water from the upstream EBPR process. The culture composition did not change throughout the 85 days of cultivation and *Chlorella sp.* remained as a single microalgal species even though we used treated used water from the EBPR system without disinfection. There was some variation in the cell number and cell area during the cultivation (Fig. 2) that could be related to the variation in biomass concentration. However, the correlation with the TSS concentration is scattered and does not show strong relation (Fig. S7, SI). No major differences were observed in the cell counts from both PBR, suggesting the microalgae grew at similar rates in both of them. This is likely a consequence of excessive volumetric nutrient loading, which allowed *Chlorella sp.* to grow under non-limiting conditions. Indeed, only at the end of the operational period where the NPR was set to 10.3±0.3 nitrate reached levels close to 0 mg-N/L, suggesting that nitrate was not limiting during most of the operational period and *Chlorella sp.* grew at maximum capacity during most of the operational period. We note that only *Chlorella sp.* were detected during this operational period. Grazers were not present in the influent and therefore there was not competitive advantage for *Scenedesmus sp.*, which were outcompeted by *Chlorella sp.* due to their comparably higher growth rates (Galès et al., 2019). The main difference between the two operational periods is the influent. When growing the mixed culture,

301 the effluents were collected from a lab-scale short SRT EBPR system suffering extreme filamentous
302 bulking (Valverde-Pérez et al., 2016b), while in the second case effluents were collected from a lab-
303 scale EBPR system exhibiting good performance (Valverde-Pérez 2015). Poor settleability promotes
304 the proliferation of swimming protozoa (Liu et al., 2008), which explains why predators were only
305 present in the study when the mixed culture was grown. In this experiment, the lowest NPR was
306 higher than in case of the mixed culture experiment. NPR for *Chlorella sp*. biomass composition
307 (Beuckels et al., 2015) are typically higher than for diatoms (Garcia et al., 2018) and therefore, a
308 proper control of the NPR could effectively keep *Chlorella sp*. culture stable in the PBR. Thus
309 controlling the NPR is a powerful tool to regulate and stabilize PBR used for resource recovery in
310 combination with bacterial systems designed for carbon capture at low SRTs, as it is the case for the
311 TRENS system (Valverde-Pérez et al., 2016a).

312 **<Figure 2>**

313 These results also demonstrate image analysis as a powerful tool to monitor algal system
314 performance. This is especially relevant for open pond systems, which are usually subject to
315 contamination by algae and other microbes (Montemezzani et al., 2015). Similar tools have been
316 designed for activated sludge systems to, e.g., monitor filamentous bulking, and successfully
317 implemented in full-scale systems (Mesquita et al., 2013). However, the application of these tools for
318 microalgal cultures is limited to cell counting and morphology characterization, without
319 distinguishing among species in mixed cultures (Havlik et al., 2013). More complex monitoring tools
320 working at different wavelengths can perform similar measurements to those presented in our work
321 (Winckelmann et al., 2016). However, to the best of our knowledge, no studies have used field
322 microscopy combined with image analysis tools to characterize microalgal composition in mixed
323 cultures. The method developed in this study has the potential to be implemented in full-scale algal

systems, offering new controlled variables, e.g. algal diversity, thereby leading to the development of innovative control strategies beyond conventional pH or cell density control (Olivieri et al., 2014).

3.2. Impact of influent NPR on treatment efficiency and nutrient recovery

The nutrients removal and effluent quality of the PBRs were assessed during the cultivation of mixed microalgal consortium (Fig. 3, Fig. S8, SI) and through the cultivation of the *Chlorella sp.* monoculture. As for the cultivation of the mixed microalgal consortium, the phosphate removal decreased significantly, from 95% to 40%, as a result of decreasing influent NPR, likely due to nitrogen limitation. Once the cultivation conditions were restored, the removal for both nitrogen and phosphorus reached up to 95%. The effluent quality was significantly affected by the changes in microalgal composition as a result of changes in influent NPR (Fig. S8, SI). The biomass concentration and the soluble effluent nitrogen concentration decreased during the NPR=5.2 period, while the effluent soluble phosphate concentration increased (Fig. S8, SI). Phosphorus quota reached a maximum of 0.15 g-P/g-TSS and was kept stable during the operational period, suggesting nitrogen was the limiting factor for biomass growth. Similar to our previous observations with the mixed culture, the nitrogen quota shows high variability (Wágner et al., 2016b). Interestingly, the pigments concentrations were not considerably affected by the change of NPR (Fig. S9, SI). Nevertheless, chlorophyll concentration showed high variability until day 10, which made it difficult to demonstrate that reduced NPR yielded low chlorophyll content. It should be noted that once the NPR was restored in day 10.5, chlorophyll content was more stable and always above 2.5 mg-chlorophyll/g-TSS. Previous studies demonstrated that under low nitrogen feeding conditions, such as those when the PBR was operated with NPR=5.2, can yield to lower chlorophyll content (Wágner et al., 2018).

<Figure 3>

346 In the cultivation of the *Chlorella sp.* monoculture, no significant difference was observed in the TSS
347 concentration (Fig. 4a) in R1 and R2, except for the NPR=10.3±0.3 for R2, where biomass
348 concentration was slightly lower in R2 (0.09 g/L) by the end of the period. Compared to the reference
349 reactor with constant nutrient supply (R1), in R2, during the period of decreased nutrient availability
350 (NPR=10.3±0.3), the nitrate concentration decreased until a steady-state at 1 mg N/L (Fig. 4d), lower
351 than R1, whilst the internal nitrogen cell quota decreased to 0.01 gN/gCOD below that of R1 in the
352 beginning of the low NPR period (Fig. 4b). During the phase of excess nutrient supply
353 (NPR=25.8±1.7), there was an increase of the nitrate concentration in R2 until a steady state at 23 mg
354 N/L, higher than R1, and an increase of the internal cell quota (0.12 gN/gCOD), higher than R1. This
355 is reflected in the removal of nitrate (Fig. 4f). On average there was 75% nitrogen removal that
356 increased to 95% under 10.3±.3 NPR and decreased to 60% under 25.8±1.7 NPR. The phosphate and
357 the internal phosphorus quota (Fig. 4 e and c) showed no difference between the two reactor
358 operations, resulting in a 60% average removal (Fig. 4f). Since phosphorus was not fully removed
359 during the experiment, probably, the phosphorus load was too high and SRT and HRT too low during
360 this experiment, thus limiting P removal. Nitrate accumulated in the last period, suggesting that
361 feeding load was above the optimal range of NPR. The pigment content was not significantly affected
362 by the change of NPR as no difference was observed between R1 and R2 (Fig. S10, SI), possibly
363 because algae were not nutrient starved long enough.

364 **<Figure 4>**

365 In the beginning of the operating period with influent NPR=10.3±0.3, a decrease of nitrogen quota in
366 R2 was observed, whilst TSS concentration remained unchanged. This result suggests that algae were
367 able to grow under nitrogen limiting conditions at the expense of their internal nitrogen quota. In the
368 second half of the NPR =10.3±0.3 period, the biomass concentration decreased in R2 while the
369 nitrogen quota replenished. Hence, we conclude that the growth rate may not be affected by changes

in the influent NPR lasting for only a few days. Thus, the control by Valverde-Pérez et al. (2016a) will allow stable and optimal algal cultivation. Furthermore, sub-optimal NPR ratios may not result in growth rate limitation as long as both nitrogen and phosphorus are fed in-excess concentrations at a given SRT, as suggested by Arbib et al. (Arbib et al., 2013). However, if one of the nutrients becomes limiting for the given operational conditions, algal biomass productivity is considerably reduced. The NPR inside the algae was calculated (Fig. 5a) and it was found to be varying between 2.7 – 21.4 mol N/mol P. This range of NPR was obtained when nitrogen was varied and might expand when phosphorus is varied as well. The calculated protein content of the algae (calculated by direct conversion from the nitrogen quota) is between 0.06 – 0.8 g protein/g DW (Fig. 5b) and it is around 0.4 g protein/g DW under optimal NPR operation. This is in agreement with literature where Rasouli et al. (2018) reported 45% protein content for *Chlorella sorokiniana* and Molazadeh et al. (2019) reported between 43-61% protein content for *Chlorella vulgaris*. The high protein is, indeed, comparable to other microbial protein sources, such as methanotrophic bacteria (Valverde-Pérez et al., 2020).

<Figure 5>

3.3. Effect of influent NPR on microalgal growth kinetics

3.3.1. Changes in microalgal culture composition

To assess the impact of alteration in the influent nutrient supply to PBRs, the average parameter set reported in Wágner et al. (2016b) was used to simulate the results obtained in the continuous reactor operation with the mixed consortium. When only *Chlorella* and *Scenedesmus sp*. were present in the culture, accurate prediction of the biomass concentration, the nitrogen and phosphorus internal cell quota and the soluble nitrogen and phosphorus species were obtained (Fig. 6). When the influent NPR was lowered to 5.2 and diatoms and other microbes proliferated in the culture, the simulations failed

393 to predict the measured data. This discrepancy between measured and predicted results indicates
394 altered process kinetics as a result of the diatom invasion, and the consequent deterioration of nutrient
395 recovery in the PBR. Some discrepancies exist for the internal nitrogen quota, which can be
396 consequence of a potential change in the nitrogen storage kinetics after the nitrogen limitation. The
397 latter phenomenon was also observed by Wágner et al. (2016b).

398 **<Figure 6>**

399 *3.3.2 Model calibration and evaluation of the operation with Chlorella sp.*

400 The batch reactors were used to estimate kinetic parameters of the ASM-A model (Fig. S11 - S13,
401 SI). The half-saturation coefficient and maximum uptake rate of nitrogen and phosphorus ($K_{NO,Alg}$,
402 $K_{PO,Alg}$, $k_{NO,Alg}$ and $k_{PO,Alg}$),the maximum specific growth rate ($\mu_{A,max}$) and the biomass decay rate (b_{Alg})
403 were estimated using the LHSS method. Since the ammonium concentration in the PBR was low
404 (below 0.1 mg/L) during the reactor operation as nitrate was the nitrogen source, $K_{NH,Alg}$ and $k_{NH,Alg}$
405 were not estimated in this experiment and literature value from Wágner et al. (2016b) was used. The
406 estimated parameter subsets do not show significant differences obtained for the three batch
407 experiments (Table 1).

408 **<Table 1>**

409 Using the estimated parameter set obtained in the batch that was conducted after the first period with
410 NPR=16.8±2 (17-17 batch, Table 1) we assessed the model prediction accuracy of the other two
411 batches using the Janus coefficient (Table S3, SI). We found J~1, suggesting that the parameter set
412 was fit to predict the PBR performance in the full operation period. Indeed, comparably good fit is
413 obtained with the simulation results throughout the 85 days of experiments (Fig. 7) in terms of
414 microalgal biomass concentration, soluble nitrate and phosphate concentration and internal
415 phosphorus quota. The decrease of internal nitrogen quota in the beginning of the NPR= 10.3±0.3

period was not captured by the model prediction. In the same period, biomass concentration is slightly over-predicted, possibly due to error propagation from the internal nitrogen quota predictions. This was the only period where algae suffered nitrogen limitation. When dynamics expose algae to nitrogen limitation conditions the maximum nitrate uptake rate ($k_{NO,Alg}$) shows variability (Wágner et al., 2016b) and therefore a recalibration of that parameter would have been needed for proper prediction of that period. When the algae was not under stress condition, no change in the kinetics for the monoculture is observed. Taken together, the ASM-A simulation model can predict PBR performance under dynamic conditions as long as there is no extreme nutrient limitation, which heavily affects nitrate uptake rates or no changes the microbial composition of the consortium which affects the biokinetics.

<Figure 7>

4. Conclusions

Effects of varying NPR on microalgal cultivation in terms of microbial composition and process performance was assessed when cultivated on used water resources. During the cultivation of the mixed microalgal species, diatoms, an indigenous alga, proliferated in the reactor when the NPR was lowered below the optimal NPR range, and they were outcompeted once the NPR was restored. Changes in microbial community could be effectively tracked by an image analysis method, which has the potential of being a monitoring tool for full-scale algal systems. The phosphate removal decreased significantly, after the NPR was lowered in the influent but once the cultivation conditions were restored for the seeded green microalgal species, the removal for both nitrogen and phosphorus recovered. Biomass and nitrogen concentration decreased while phosphorus concentration increased in the effluent by decreasing the NPR. The ASM-A model could capture the measured data under

optimal NPR operation, but it failed to predict the measured results when diatoms proliferated under low NPR.

A monoculture of *Chlorella sp.* cultivated on used water resources with varying NPR remained stable and contamination-free. Low NPR condition decreased the biomass concentration, effluent nitrogen concentration and the internal nitrogen quota. The ASM-A model was calibrated for this monoculture and model simulations could predict the measurement data in continuous operation using a single parameter subset. Under nutrient limitation conditions, which affects the nitrate uptake rates, the model could not predict the nitrogen quota.

This study demonstrates that NPR is a powerful control parameter of the PBR performance. Moreover, process configurations or control schemes reported in literature (see, e.g. Valverde-Pérez et al. (2016a)) could effectively optimize the PBR performance.

Acknowledgements

Dorottya Wágner thanks the European Commission, (E4WATER Project, FP7-NMP-2011.3.4-1 grant agreement 280756) for the funding. Borja Valverde-Pérez thanks the Integrated Water Technology (InWaTech) project (http://www.inwatech.org) for the financial support.

CRediT author statement

Dorottya S. Wágner: conceptualization, methodology, investigation, formal analysis, software, data curation, visualization, writing – original draft preparation. **Clarissa Cazzaniga:** conceptualization, investigation, data curation. **Michael Steidl:** conceptualization, investigation, data curation. **Arnaud Dechesne:** methodology, supervision, formal analysis, writing – review & editing. **Borja Valverde-**

458 **Pérez:** conceptualization, investigation, software, writing – review & editing. **Benedek Gy. Plósz:**
459 conceptualization, supervision, writing – review & editing.

460 Conflict of interest statement

461 The authors declare that there are no known conflicts of interest associated with this publication.

462 Statement of informed consent, human/animal rights

463 No conflicts, informed consent, human or animal rights applicable.

464 Declaration of authors agreement to authorship

465 The work described has not been published previously and it is not under consideration for publication
466 elsewhere. The publication and submission of the manuscript for peer review is approved by all
467 authors.

468 References

469 Alcántara, C., Domínguez, J.M., García, D., Blanco, S., Pérez, R., García-Encina, P.A., Muñoz, R.,
470 2015. Evaluation of wastewater treatment in a novel anoxic-aerobic algal-bacterial
471 photobioreactor with biomass recycling through carbon and nitrogen mass balances. Bioresour.
472 Technol. 191, 173–186.

473 Anbalagan, A., Schwede, S., Lindberg, C.F., Nehrenheim, E., 2016. Influence of hydraulic retention
474 time on indigenous microalgae and activated sludge process. Water Res. 91, 277–284.

475 APHA, American Water Works Association, Water Environment Federation, 1999. Standard
476 methods for the examination of water and wastewater, Standard Methods. Washington DC.

477 Arbib, Z., Ruiz, J., Alvarez-Diaz, P., Garrido-Perez, C., Barragan, J., Perales, J.A., 2013.
478 Photobiotreatment: influence of nitrogen and phosphorus ratio in wastewater on growth
479 kinetics of *Scenedesmus obliquus*. Int J Phytoremediation 15, 774–788.

480 Batstone, D.J., Hülsen, T., Mehta, C.M., Keller, J., 2015. Platforms for energy and nutrient recovery
481 from domestic wastewater: A review. Chemosphere 140, 2–11.

https://doi.org/10.1016/j.chemosphere.2014.10.021

Béchet, Q., Shilton, A., Guieysse, B., 2016. Maximizing Productivity and Reducing Environmental Impacts of Full-Scale Algal Production through Optimization of Open Pond Depth and Hydraulic Retention Time. Environ. Sci. Technol. 50, 4102–4110.

Beuckels, A., Smolders, E., Muylaert, K., 2015. Nitrogen availability influences phosphorus removal in microalgae-based wastewater treatment. Water Res. 77, 98–106.

Boelee, N.C., Temmink, H., Janssen, M., Buisman, C.J.N., Wijffels, R.H., 2011. Nitrogen and phosphorus removal from municipal wastewater effluent using microalgal biofilms. Water Res. 45, 5925–5933.

Borowitzka, M.A., Moheimani, N.R., n.d. Algae for Biofuels and Energy.

Cai, T., Park, S.Y., Li, Y., 2013. Nutrient recovery from wastewater streams by microalgae: Status and prospects. Renew. Sustain. Energy Rev. 19, 360–369. https://doi.org/10.1016/j.rser.2012.11.030

Coppens, J., Grunert, O., Van Den Hende, S., Vanhoutte, I., Boon, N., Haesaert, G., De Gelder, L., 2016. The use of microalgae as a high-value organic slow-release fertilizer results in tomatoes with increased carotenoid and sugar levels. J. Appl. Phycol. 28, 2367–2377. https://doi.org/10.1007/s10811-015-0775-2

Dang, H., Hall, E., Lovejoy, C., Ptacnik, R., Yvon-Durocher, G., Martiny, A.C., Garcia, N.S., Sexton, J., Riggins, T., Brown, J., Lomas, M.W., 2018. High Variability in Cellular Stoichiometry of Carbon, Nitrogen, and Phosphorus Within Classes of Marine Eukaryotic Phytoplankton Under Sufficient Nutrient Conditions. Front. Microbiol. | www.frontiersin.org 1, 543. https://doi.org/10.3389/fmicb.2018.00543

De Francisci, D., Su, Y., Iital, A., Angelidaki, I., 2018. Evaluation of microalgae production coupled with wastewater treatment. Environ. Technol. 39, 581–592.

Dickinson, K.E., Whitney, C.G., McGinn, P.J., 2013. Nutrient remediation rates in municipal wastewater and their effect on biochemical composition of the microalga *Scenedesmus sp.* AMDD. Algal Res. 2, 127–134.

Fan, C., Glibert, P.M., Burkholder, J.A.M., 2003. Characterization of the affinity for nitrogen, uptake kinetics, and environmental relationships for Prorocentrum minimum in natural blooms and laboratory cultures. Harmful Algae 2, 283–299. https://doi.org/10.1016/S1568-9883(03)00047-7

Fang, L.L., Valverde-Pérez, B., Damgaard, A., Plósz, B.G., Rygaard, M., 2016. Life cycle assessment as development and decision support tool for wastewater resource recovery technology. Water Res. 88, 538–549.

Galès, A., Bonnafous, A., Carré, C., Jauzein, V., Lanouguère, E., Le Floc'h, E., Pinoit, J., Poullain, C., Roques, C., Sialve, B., Simier, M., Steyer, J.P., Fouilland, E., 2019. Importance of ecological interactions during wastewater treatment using High Rate Algal Ponds under different temperate climates. Algal Res. 40, 101508. https://doi.org/10.1016/j.algal.2019.101508

521 Gao, H., Scherson, Y.D., Wells, G.F., 2014. Towards energy neutral wastewater treatment:
522 methodology and state of the art. Environ. Sci. Process. impacts 16, 1223–1246.

523 Garcia, N.S., Sexton, J., Riggins, T., Brown, J., Lomas, M.W., Martiny, A.C., 2018. High
524 variability in cellular stoichiometry of carbon, nitrogen, and phosphorus within classes of
525 marine eukaryotic phytoplankton under sufficient nutrient conditions. Front. Microbiol. 9, 1–
526 10.

527 Gardner-Dale, D.A., Bradley, I.M., Guest, J.S., 2017. Influence of solids residence time and carbon
528 storage on nitrogen and phosphorus recovery by microalgae across diel cycles. Water Res. 121,
529 231–239. https://doi.org/10.1016/J.WATRES.2017.05.033

530 Geider, R.J., La Roche, J., 2002. Redfield revisited: Variability of C:N:P in marine microalgae and
531 its biochemical basis. Eur. J. Phycol. https://doi.org/10.1017/S0967026201003456

532 Geiss, R.H., Rice, K.P., Keller, R.R., Chen, G., Zhao, L., Qi, Y., 2015. Enhancing the productivity
533 of microalgae cultivated in wastewater toward biofuel production: A critical review. Appl.
534 Energy 137, 282–291.

535 Havlik, I., Lindner, P., Scheper, T., Reardon, K.F., 2013. On-line monitoring of large cultivations of
536 microalgae and cyanobacteria. Trends Biotechnol. 31, 406–414.
537 https://doi.org/10.1016/j.tibtech.2013.04.005

538 Henze, M., Van Loosdrecht, M.C.M., Ekama, G.A., Brdjanovic, D., 2008. Biological wastewater
539 treatment : principles, modelling and design. IWA Publishing, UK.

540 Ikaran, Z., Suárez-Alvarez, S., Urreta, I., Castañón, S., 2015. The effect of nitrogen limitation on
541 the physiology and metabolism of Chlorella vulgaris var L3. Algal Res. 10, 134–144.

542 Krustok, I., Odlare, M., Shabiimam, M.A., Truu, J., Truu, M., Ligi, T., Nehrenheim, E., 2015.
543 Characterization of algal and microbial community growth in a wastewater treating batch
544 photo-bioreactor inoculated with lake water. Algal Res. 11, 421–427.
545 https://doi.org/10.1016/j.algal.2015.02.005

546 Liu, J., Vyverman, W., 2015. Differences in nutrient uptake capacity of the benthic filamentous
547 algae *Cladophora sp.*, *Klebsormidium sp.* and *Pseudanabaena sp.* under varying N/P
548 conditions. Bioresour. Technol. 179, 234–242.

549 Liu, J., Yang, M., Qi, R., An, W., Zhou, J., 2008. Comparative study of protozoan communities in
550 full-scale MWTPs in Beijing related to treatment processes. Water Res. 42, 1907–1918.
551 https://doi.org/10.1016/j.watres.2007.11.020

552 Lynch, F., Santana-Sánchez, A., Jämsä, M., Sivonen, K., Aro, E.M., Allahverdiyeva, Y., 2015.
553 Screening native isolates of cyanobacteria and a green alga for integrated wastewater
554 treatment, biomass accumulation and neutral lipid production. Algal Res. 11, 411–420.

555 Marcilhac, C., Sialve, B., Pourcher, A.M., Ziebal, C., Bernet, N., Béline, F., 2015. Control of
556 nitrogen behaviour by phosphate concentration during microalgal-bacterial cultivation using
557 digestate. Bioresour. Technol. 175, 224–230.

558 Mata, T.M., Martins, A.A., Caetano, N.S., 2010. Microalgae for biodiesel production and other
559 applications: A review. Renew. Sustain. Energy Rev. 14, 217–232.

560 Matassa, S., Batstone, D.J., Hülsen, T., Schnoor, J., Verstraete, W., 2015. Can direct conversion of
561 used nitrogen to new feed and protein help feed the world? Environ. Sci. Technol. 49, 5247–
562 5254.

563 Mayers, J.J., Flynn, K.J., Shields, R.J., 2014. Influence of the N: P supply ratio on biomass
564 productivity and time-resolved changes in elemental and bulk biochemical composition of
565 *Nannochloropsis sp.* Bioresour. Technol. 169, 588–595.

566 Mehta, C.M., Khunjar, W.O., Nguyen, V., Tait, S., Batstone, D.J., 2015. Technologies to recover
567 nutrients from waste streams: A critical review. Crit. Rev. Environ. Sci. Technol. 45, 385–427.

568 Mesquita, D.P., Amaral, A.L., Ferreira, E.C., 2013. Activated sludge characterization through
569 microscopy: A review on quantitative image analysis and chemometric techniques. Anal.
570 Chim. Acta 802, 14–28. https://doi.org/10.1016/J.ACA.2013.09.016

571 Miralto, A., Barone, G., Romano, G., Poulet, S.A., Ianora, A., Russo, G.L., Buttino, I., Mazzarella,
572 G., Laablr, M., Cabrini, M., Glacobbe, M.G., 1999. The insidious effect of diatoms on copepod
573 reproduction. Nature 402, 173–176. https://doi.org/10.1038/46023

574 Molazadeh, M., Danesh, S., Ahmadzadeh, H., Pourianfar, H.R., 2019. Influence of CO2
575 concentration and N:P ratio on Chlorella vulgaris-assisted nutrient bioremediation, CO2
576 biofixation and biomass production in a lagoon treatment plant. J. Taiwan Inst. Chem. Eng. 96,
577 114–120.

578 Montemezzani, V., Duggan, I.C., Hogg, I.D., Craggs, R.J., 2015. A review of potential methods for
579 zooplankton control in wastewater treatment High Rate Algal Ponds and algal production
580 raceways. Algal Res. 11, 211–226.

581 Novoveská, L., Franks, D.T., Wulfers, T.A., Henley, W.J., 2016. Stabilizing continuous mixed
582 cultures of microalgae. Algal Res. 13, 126–133.

583 Olivieri, G., Salatino, P., Marzocchella, A., 2014. Advances in photobioreactors for intensive
584 microalgal production: configurations, operating strategies and applications. J. Chem. Technol.
585 Biotechnol. 89, 178–195. https://doi.org/10.1002/jctb.4218

586 Powell, N., Shilton, A., Pratt, S., Chisti, Y., 2011. Luxury uptake of phosphorus by microalgae in
587 full-scale waste stabilisation ponds. Water Sci. Technol. 63, 704–709.

588 Rasouli, Z., Valverde-Pérez, B., D'Este, M., De Francisci, D., Angelidaki, I., 2018. Nutrient
589 recovery from industrial wastewater as single cell protein by a co-culture of green microalgae
590 and methanotrophs. Biochem. Eng. J. 134, 129–135.
591 https://doi.org/10.1016/J.BEJ.2018.03.010

592 Redfield, A.C., 1958. The Biological Control of Chemical Factors in the Environment. Am. Sci. 46,
593 205–221.

594 Rhee, G.-Y., 1978. Effects of N:P atomic ratios nitrate limitation on algal growth, cell composition,
595 nitrate uptake. Limnol. Oceanogr. 23, 10–25.

596 Rhee, G.-Y., Gotham, I.J., 1980. Optimum N:P Ratios and Coexistence of Planktonic Algae. J.
597 Phycol. 16, 486–489.

598 Safafar, H., Wagenen, J. Van, Møller, P., Jacobsen, C., 2015. Carotenoids, phenolic compounds and
599 tocopherols contribute to the antioxidative properties of some microalgae species grown on
600 industrial wastewater. Mar. Drugs 13, 7339–7356.

601 Sforza, E., Ramos-Tercero, E.A., Gris, B., Bettin, F., Milani, A., Bertucco, A., 2014. Integration of
602 *Chlorella protothecoides* production in wastewater treatment plant: From lab measurements to
603 process design. Algal Res. 6, 223–233.

604 Sin, G., De Pauw, D.J.W., Weijers, S., Vanrolleghem, P.A., 2008. An efficient approach to
605 automate the manual trial and error calibration of activated sludge models. Biotechnol. Bioeng.
606 100, 516–528. https://doi.org/10.1002/BIT.21769

607 Solovchenko, A., Verschoor, A.M., Jablonowski, N.D., Nedbal, L., 2016. Phosphorus from
608 wastewater to crops: An alternative path involving microalgae. Biotechnol. Adv.
609 https://doi.org/10.1016/j.biotechadv.2016.01.002

610 Sutherland, D.L., Turnbull, M.H., Craggs, R.J., 2014. Increased pond depth improves algal
611 productivity and nutrient removal in wastewater treatment high rate algal ponds. Water Res.
612 53, 271–281.

613 Templeton, D.W., Laurens, L.M.L., 2015. Nitrogen-to-protein conversion factors revisited for
614 applications of microalgal biomass conversion to food, feed and fuel. Algal Res. 11, 359–367.
615 https://doi.org/10.1016/J.ALGAL.2015.07.013

616 Valverde-Pérez, B., 2015. Wastewater resource recovery via the Enhanced Biological Phosphorus
617 Removal and Recovery (EBP2R) process coupled with green microalgae cultivation. Technical
618 University of Denmark, Kgs. Lyngby, Denmark.

619 Valverde-Pérez, Borja, Fuentes-Martínez, J.M., Flores-Alsina, X., Gernaey, K. V., Huusom, J.K.,
620 Plósz, B.G., 2016a. Control structure design for resource recovery using the enhanced
621 biological phosphorus removal and recovery (EBP2R) activated sludge process. Chem. Eng. J.
622 296, 447–457. https://doi.org/10.1016/j.cej.2016.03.021

623 Valverde-Pérez, B., Ramin, E., Smets, B.F., Plósz, B.G., 2015. EBP2R - an innovative enhanced
624 biological nutrient recovery activated sludge system to produce growth medium for green
625 microalgae cultivation. Water Res. 68, 821–830.

626 Valverde-Pérez, Borja, Wágner, D.S., Lóránt, B., Gülay, A., Smets, B.F., Plósz, B.G., 2016b. Short-
627 sludge age EBPR process – Microbial and biochemical process characterisation during reactor
628 start-up and operation. Water Res. 104, 320–329. https://doi.org/10.1016/j.watres.2016.08.026

629 Valverde-Pérez, B., Xing, W., Zachariae, A.A., Skadborg, M.M., Kjeldgaard, A.F., Palomo, A.,
630 Smets, B.F., 2020. Cultivation of methanotrophic bacteria in a novel bubble-free membrane
631 bioreactor for microbial protein production. Bioresour. Technol. 310, 123388.
632 https://doi.org/10.1016/j.biortech.2020.123388

633 Van Den Hende, S., Carré, E., Cocaud, E., Beelen, V., Boon, N., Vervaeren, H., 2014. Treatment of
634 industrial wastewaters by microalgal bacterial flocs in sequencing batch reactors. Bioresour.
635 Technol. 161, 245–254.

636 Verstraete, W., Vlaeminck, S.E., 2011. ZeroWasteWater: short-cycling of wastewater resources for

637 sustainable cities of the future. Int. J. Sustain. Dev. World Ecol. 18, 253–264.

638 Wágner, D.S., Radovici, M., Smets, B.F., Angelidaki, I., Valverde-Pérez, B., Plósz, B.G., 2016a.
639 Harvesting microalgae using activated sludge can decrease polymer dosing and enhance
640 methane production via co-digestion in a bacterial-microalgal process. Algal Res. 20.
641 https://doi.org/10.1016/j.algal.2016.10.010

642 Wágner, D.S., Valverde-Pérez, B., Plósz, B.G., 2018. Light attenuation in photobioreactors and
643 algal pigmentation under different growth conditions – Model identification and complexity
644 assessment. Algal Res. 35, 488–499. https://doi.org/10.1016/j.algal.2018.08.019

645 Wágner, D.S., Valverde-Pérez, B., Sæbø, M., Bregua de la Sotilla, M., Van Wagenen, J., Smets,
646 B.F., Plósz, B.G., 2016b. Towards a consensus-based biokinetic model for green
647 microalgae – The ASM-A. Water Res. 103. https://doi.org/10.1016/j.watres.2016.07.026

648 Wang, L., Min, M., Li, Y., Chen, P., Chen, Y., Liu, Y., Wang, Y., Ruan, R., 2010. Cultivation of
649 green algae Chlorella sp. in different wastewaters from municipal wastewater treatment plant.
650 Appl. Biochem. Biotechnol. 162, 1174–1186. https://doi.org/10.1007/s12010-009-8866-7

651 Whitton, R., Le Mével, A., Pidou, M., Ometto, F., Villa, R., Jefferson, B., 2016. Influence of
652 microalgal N and P composition on wastewater nutrient remediation. Water Res. 91, 371–378.

653 Winckelmann, D., Bleeke, F., Bergmann, P., Elle, C., Klöck, G., 2016. Detection of weed algae in
654 open pond cultures of Cyanobacterium aponinum using PAM. Int. Aquat. Res. 8, 81–90.

655

656

Figures

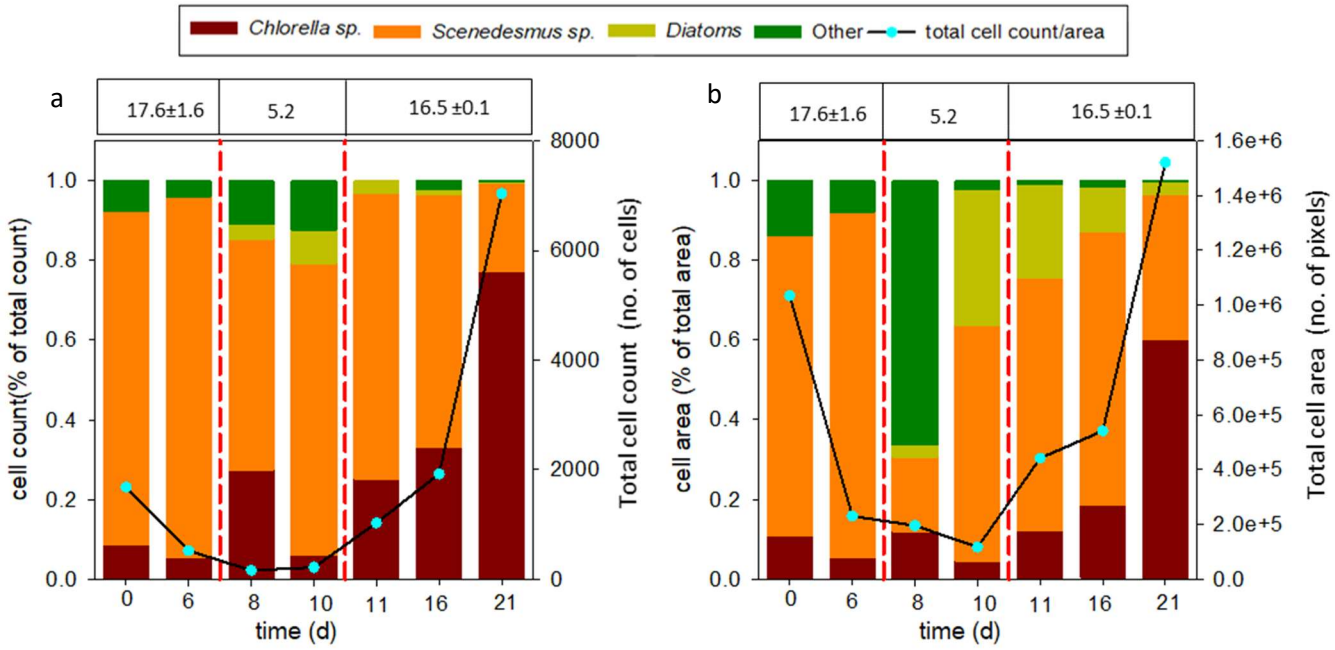

Figure 1: Variation in the culture composition during the 21 days cultivation period as affected by the NPR (indicated on the top of the graphs). (**a**) The cell counts are presented as the fraction of the total cell count. (**b**) The cell area is presented as the fraction of the total cell area (unit in pixels). The total cell count (number of cells) and the total cell area (total number of pixels per field of view) is presented on the figures, suggesting how the culture density changed.

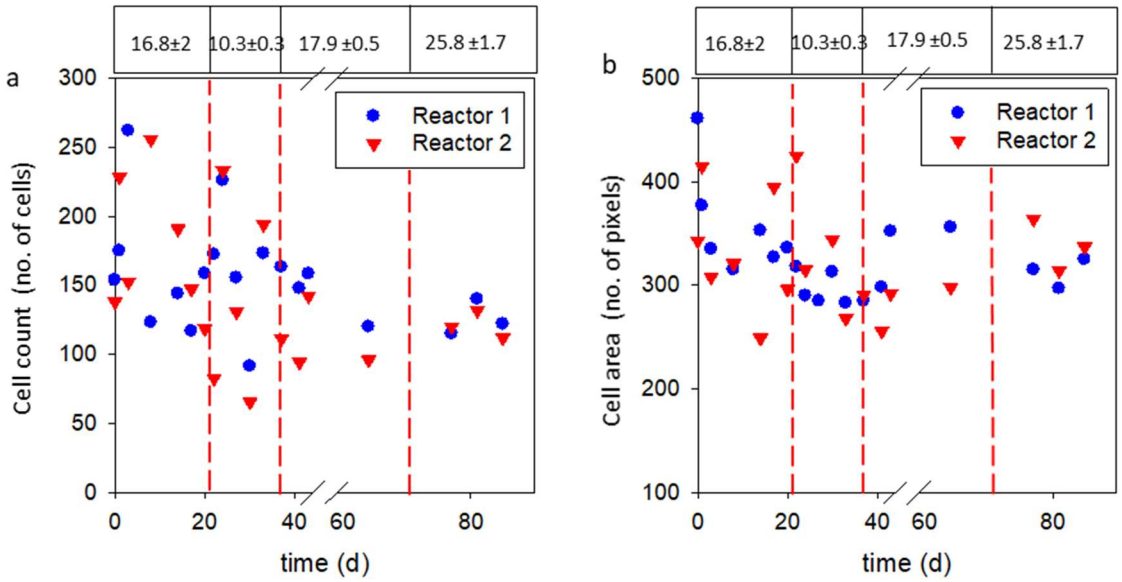

Figure 2: Total cell counts (number of cells) (**a**) and cell area (unit in pixels) (**b**) of the *Chlorella sp.* during continuous reactor operation as affected by the NPR (indicated on the top of the graphs). The gap in the x-axis refers to the period where temperature control was not applied and thus it is not considered. Reactor 1 refers to the reference reactor operated at 17.3±2 NPR whilst Reactor 2 refers to the reactor with varying NPRs.

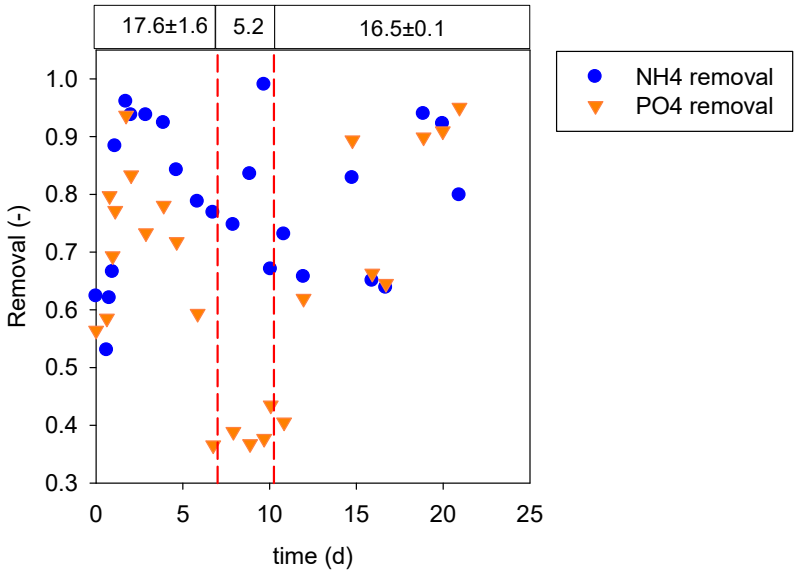

Figure 3: Removal of ammonium and phosphorus in the mixed microalgal consortium during the 21 days of cultivation (expressed as fraction of influent nutrients present in the effluent). The NPR

present in the system is indicated above the figure. The NPR (17.6±1.6, 5.2 and 16.5±0.1) is shown for each period.

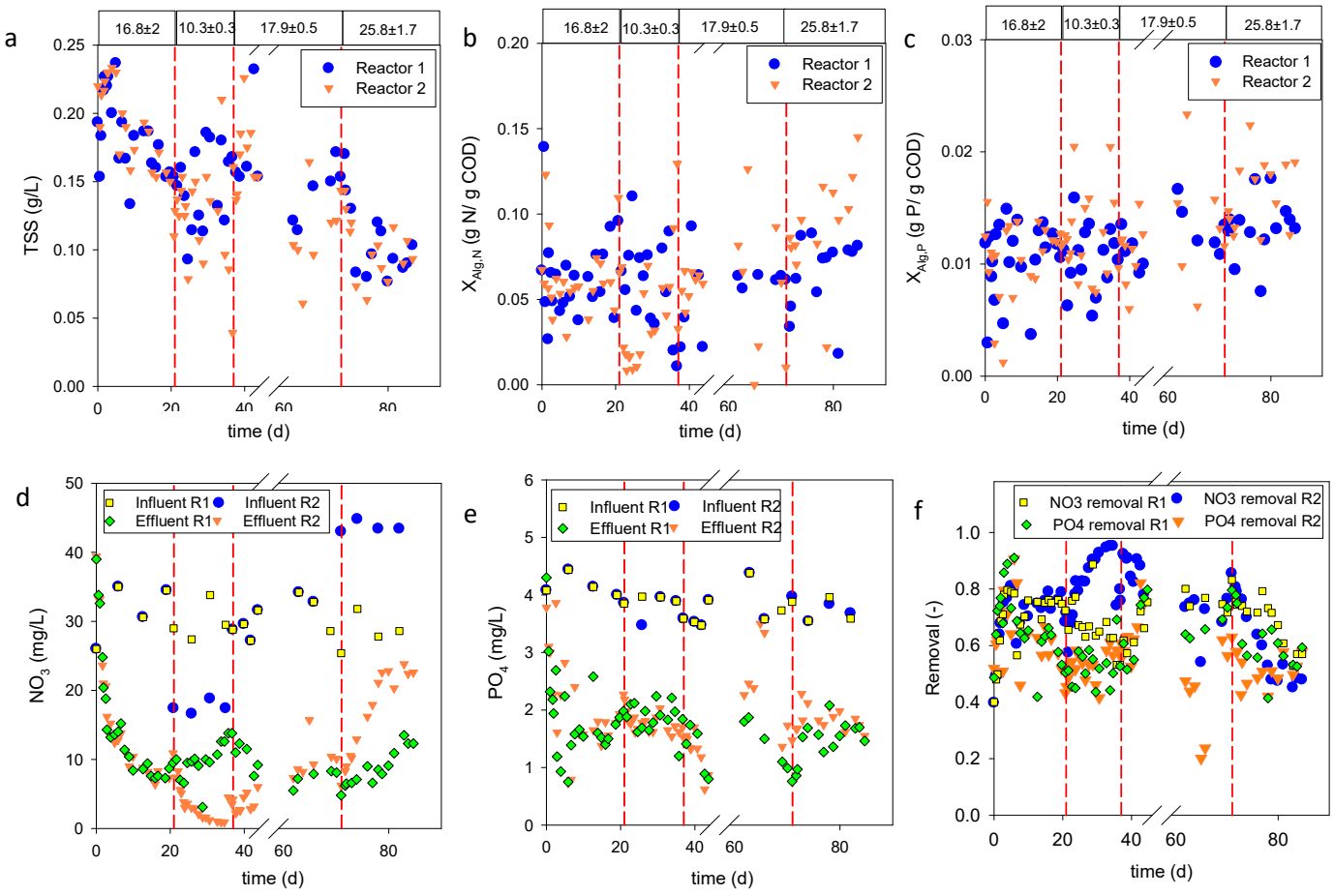

Figure 4: Biomass concentration (**a**), internal nitrogen quota (**b**), internal phosphorus quota (**c**), bulk nitrate concentration (**d**), bulk phosphate concentration (**e**), and removal of nitrogen and phosphorus (**f**) during the cultivation of *Chlorella sp.* in used water resources in Reactor 1 and 2. Reactor 1 refers to the reference reactor operated at 17.3±2 NPR whilst Reactor 2 refers to the reactor with varying NPRs.

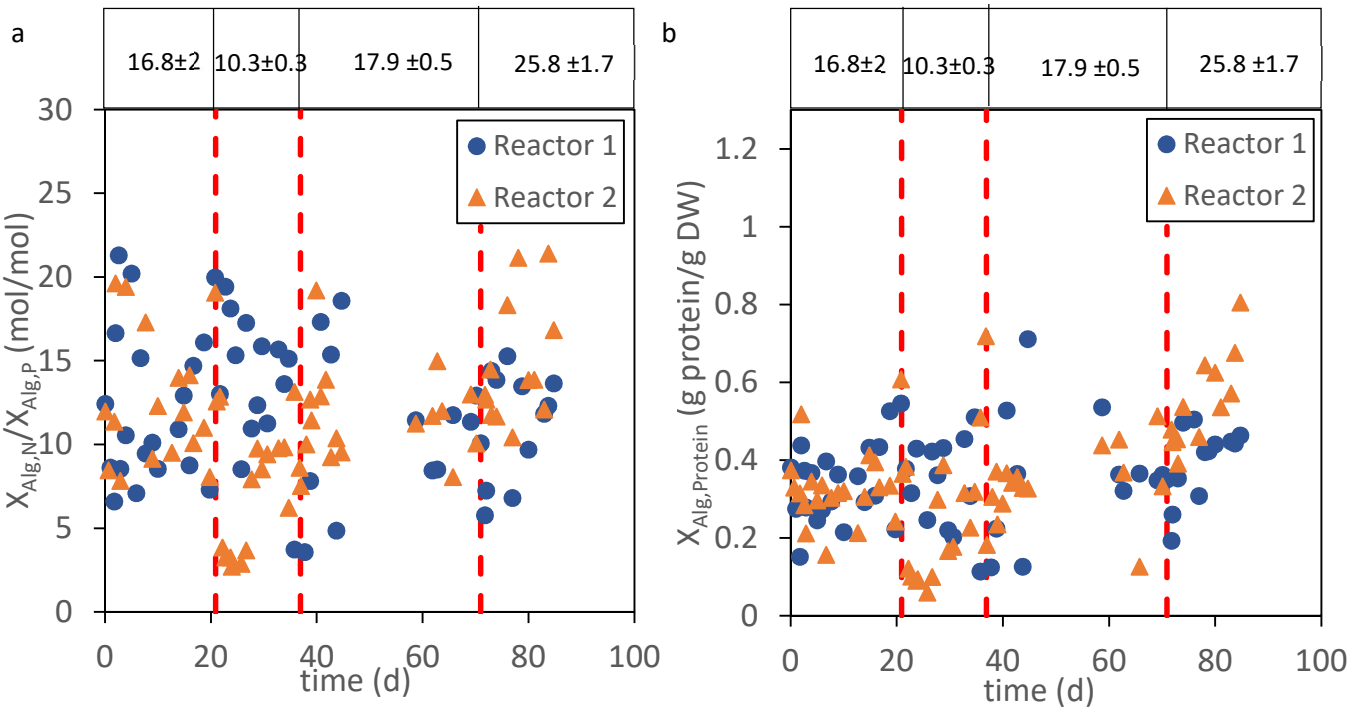

684

685 **Figure 5:** Nitrogen – to – phosphorus ratio (NPR) calculated inside the algae (**a**) and protein content
686 of the algae calculated (**b**) during the cultivation of *Chlorella sp.* in used water resources in Reactor
687 1 and 2.

688

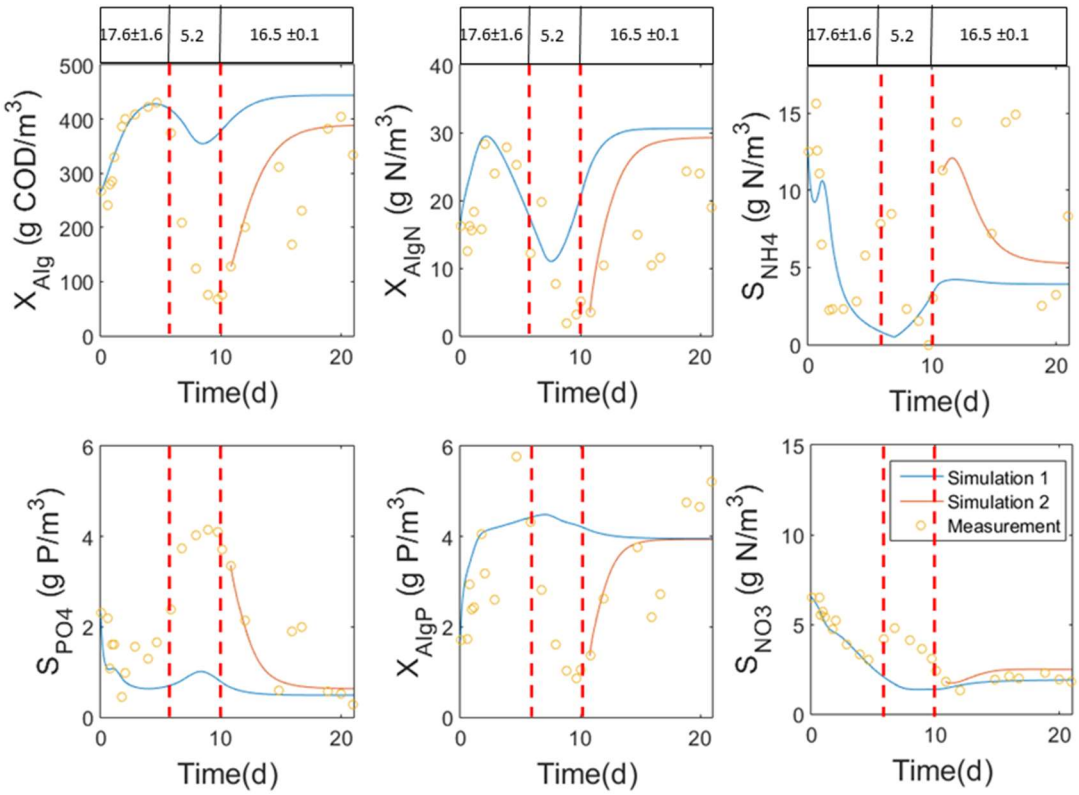

Figure 6: Simulation results of the mixed microalgal species cultivation. The red vertical dashed lines represent the time when the NPR was changed. Simulation 1 (blue line) represents the simulation of the whole cultivation period. Discrepancies following the decrease of NPR are due to the change in culture composition. Simulation 2 (orange line) represents the simulation of the second 16.5±0.1 NPR period. Discrepancies between blue and red lines are due to initial conditions after the second NPR shift, which are given by the simulation model for the full cultivation period simulation and set to the experimental values in simulation 2.

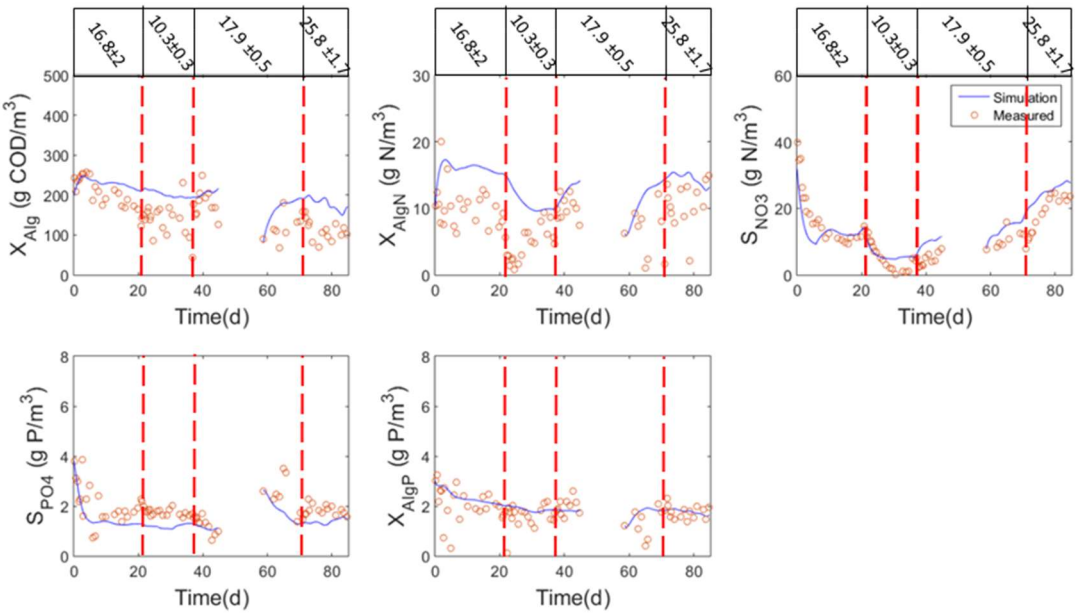

Figure 7: Simulation of Reactor 2 with varying NPR. The blue line indicates the model prediction of the measured data.

Tables

Table 1: Estimated parameter values obtained for the three batch experiments. The values are presented as mean ± standard deviation. The 17-17 batch denotes the cultivation where the inoculum was taken after the 16.8±2 NPR cultivation. The 10-17 batch denotes the cultivation where the inoculum was taken after the 10.3±0.33 NPR cultivation. The 25-17 batch denotes the cultivation where the inoculum was taken after the 25.8±1.7 NPR cultivation.

	17-17 batch	**10-17 batch**	**25-17 batch**
$\mu_{A,max}$ (d^{-1})	2.66±0.1	3.4±0.8	2.27±0.4
$K_{NO,Alg}$ (gN m^{-3})	14.55±1	13±1.4	13.7±1.8
$K_{PO,Alg}$ (gP m^{-3})	4.48±0.7	4±0.58	3.7±0.5
$k_{NO,Alg}$ (gN g^{-1}COD d^{-1})	0.14±0.02	0.1±0.02	0.14±0.05
$k_{PO,Alg}$ (gP g^{-1}COD d^{-1})	0.043±0.007	0.023±0.003	0.045±0.005
b_{Alg} (d^{-1})	0.45±0.04	0.31±0.12	0.38±0.1

Supporting Information

"Optimal influent N-to-P ratio for stable microalgal cultivation in water treatment and nutrient recovery"

Dorottya S. Wágner[*,a,b], Clarissa Cazzaniga[a], Michael Steidl[a], Arnaud Dechesne[a], Borja Valverde-Pérez[a], Benedek Gy. Plósz[*,a,c]

[a] *Department of Environmental Engineering, Technical University of Denmark, Miljøvej, Building 115, 2800 Kgs. Lyngby, Denmark*

[c] *Department of Chemical Engineering, University of Bath, Claverton Down, Bath BA2 7AY, UK*

**Corresponding authors: dsw@bio.aau.dk; bgp24@bath.ac.uk*

The supporting information contains 10 pages including: 3 tables (page S2) and 13 figures (pages S3–S9), description of the operation of the laboratory-scale continuous EBPR system (page S9), description of the calculation of TSS to COD factor (page S10).

734 **Table S1:** Initial conditions of the three batch experiments used for model calibration.

	S_{NH} (gN/m^3)	S_{NO2} (gN/m^3)	S_{NO3} (gN/m^3)	S_{PO} (gN/m^3)	X_{Nalg} (gN/m^3)	X_{Palg} (gP/m^3)	X_{Alg} ($gCOD/m^3$)
Batch 1 (17-17)	0.07	0.54	27.8	3.86	1.7	0.44	31.45036
Batch 2 (17-10)	0.37	0.12	28	3.67	0.5	0.3	67.5
Batch 3 (17-25)	0.08	0.16	28.0	3.85	1.4	0.6	26.5

735

736 **Table S2:** Settings used for automatic detection of different species during image analysis. Units
737 are in pixels.

microorganism	**area**		**aspect ratio**		**diameter**		**axis**	
	min	**max**	**min**	**max**	**min**	**max**	**min**	**max**
Chlorella sp.	50	∞	0	1.87	5	∞	0	∞
Scenedesmus sp.	50	∞	1.87	∞	0	15	0	100
Diatoms	50	∞	1.87	∞	0	15	100	∞

738

739 **Table S3:** The RMSNE and the Janus coefficient of the calibration and evaluation to assess the
740 accuracy of the model prediction.

	10-17 batch			10-25 batch		
	RMSNE calibration	RMSNE evaluation	Janus coefficient	RMSNE calibration	RMSNE evaluation	Janus coefficient
Nitrate in bulk liquid (S_{NO3})	0.3	0.83	2.76	0.3	0.3	1
Phosphate in bulk liquid (S_{PO4})	1.84	0.2	0.12	1.84	0.21	0.11
Algal biomass (X_{Alg})	0.14	0.18	1.29	0.14	0.15	1.07
Nitrogen quota (X_{AlgN})	0.24	0.36	1.5	0.24	0.18	0.75
Phosphorous quota (X_{AlgPP})	0.23	0.49	2.1	0.23	0.24	1.04
Total RMSNE	2.75	2.06	0.75	2.75	1.08	0.39

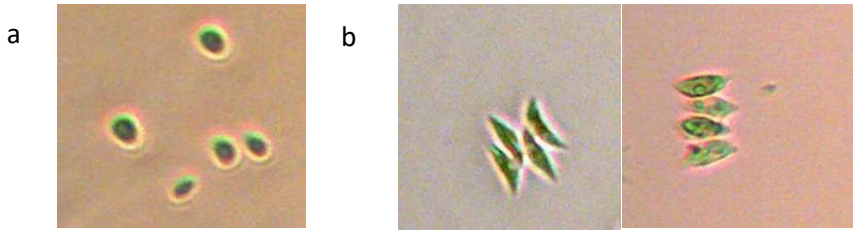

741

742 **Figure S1:** Micrographs of *Chlorella* sp. (**a**) and *Scenedesmus* sp. (**b**) used for the cultivation in this study.

743

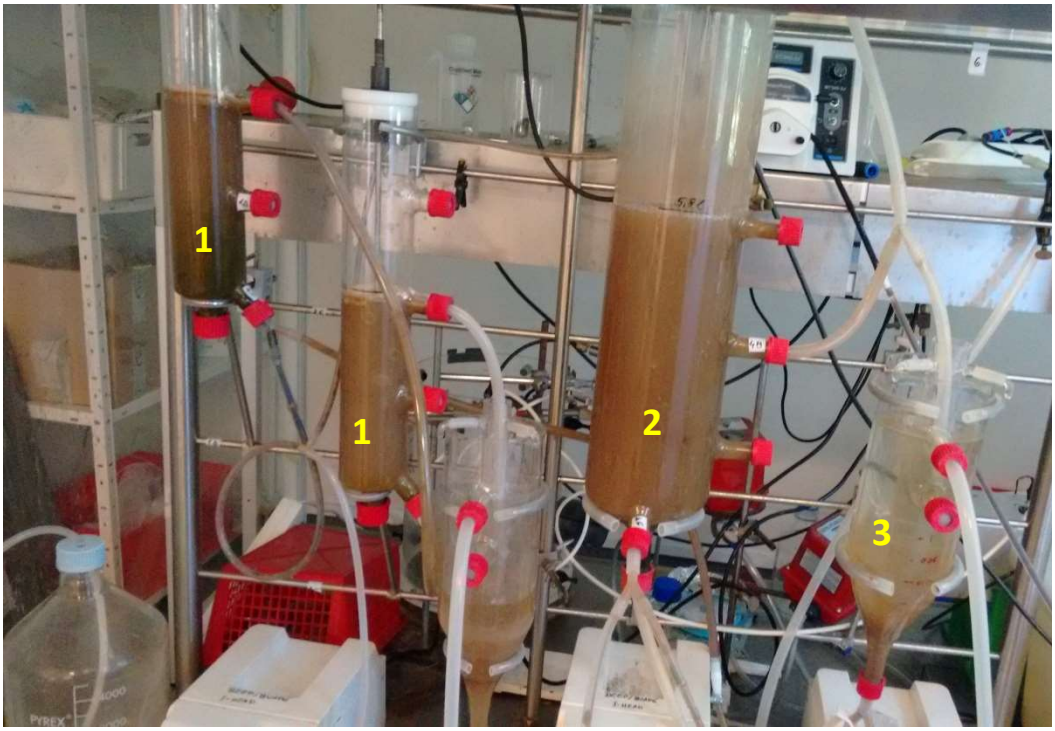

744

745 **Figure S2:** The laboratory scale EBPR system consisting of anaerobic reactors (1) an aerobic reactor (2) and
746 a solid liquid separation (3).

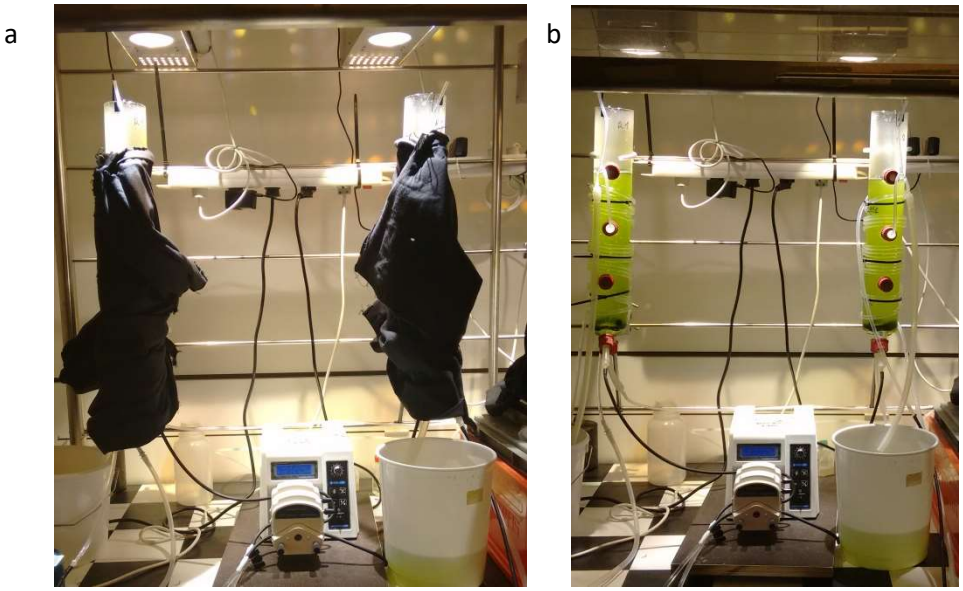

747

748 **Figure S3:** The 1.4 L continuous PBRs run in parallel for the experiments conducted with *Chlorella sp.* The
749 reactors were covered with black cloth during the operation (**a**). The reactor set-up without the black cloth
750 (**b**).

751

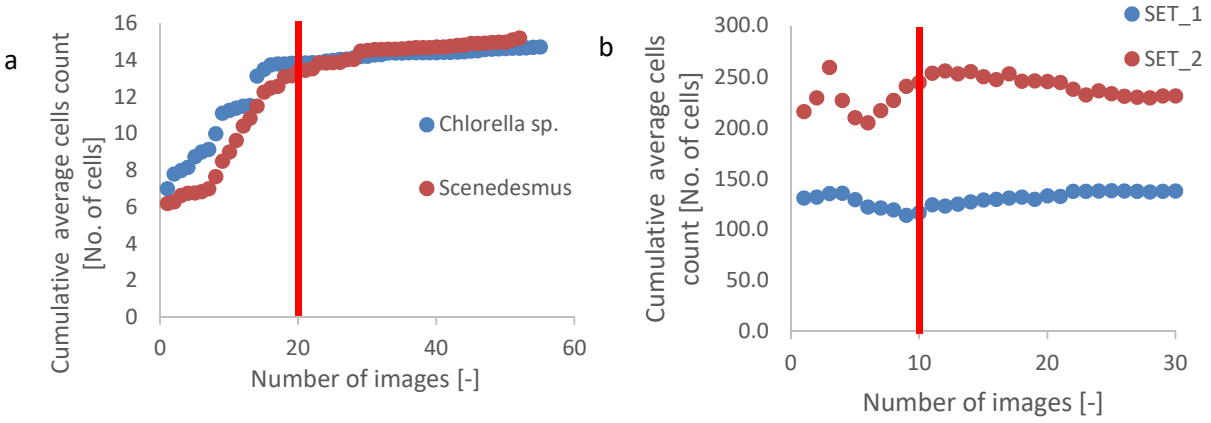

752

753 **Figure S4:** Cumulative average cells count for mixed culture of *Chlorella sp.* and *Scenedesmus sp.* (**a**)
754 Cumulative average cells count for monoculture of *Chlorella sp.* Set_1 and set_2 refer to duplicate
755 characterization of the optimal number of images, respectively. (**b**)

756

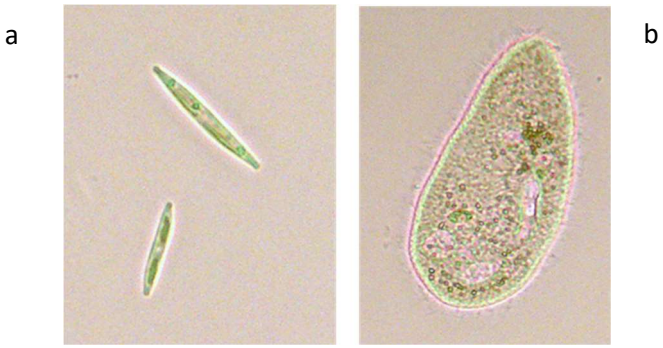

Figure S5: Diatoms, *Nitzschia sp.*(identified based on microscopy) that appeared during cultivation of the mixed consortium in the 5.2 NPR period (**a**). Ciliate that proliferated the 5.2 NPR period (**b**).

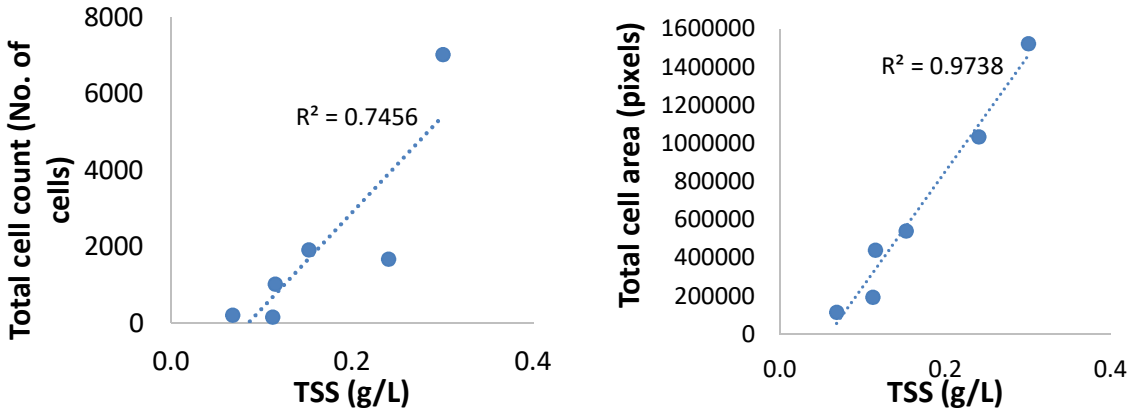

Figure S6: Correlation between the cell count and cell area during mixed microalgal cultivation.

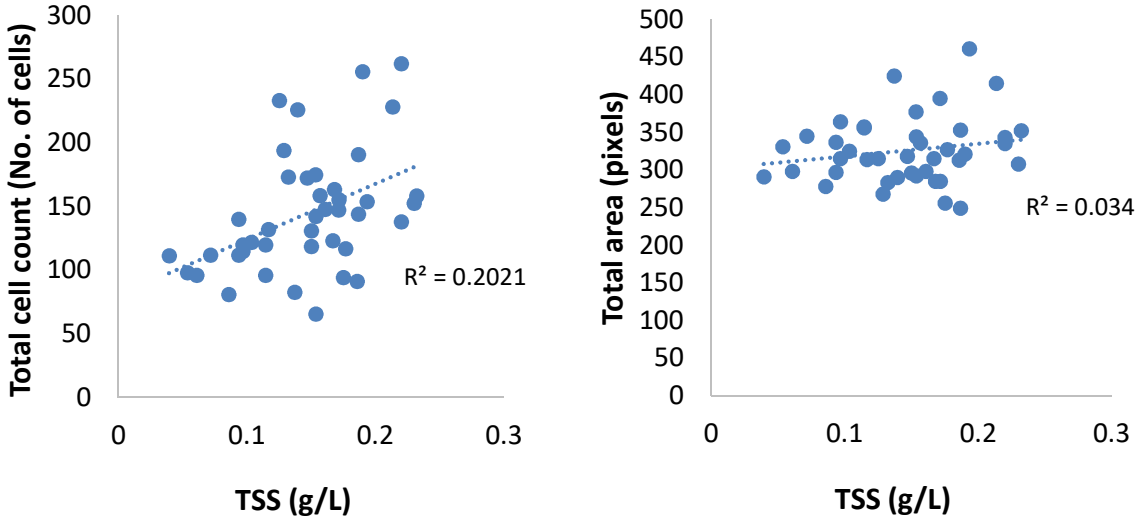

Figure S7: Correlation between the cell count and cell area during cultivation of *Chlorella sp*.

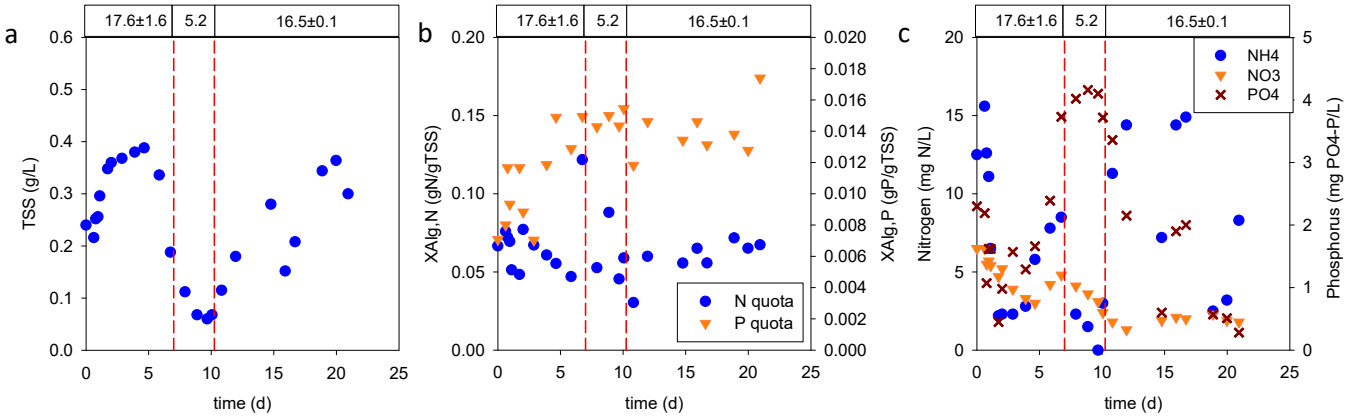

Figure S8: Biomass concentration (a), internal nitrogen quota and internal phosphorus quota (b), bulk ammonium and nitrate concentration and bulk phosphate concentration (c) during the cultivation of mixed consortium in used water resources with varying NPRs.

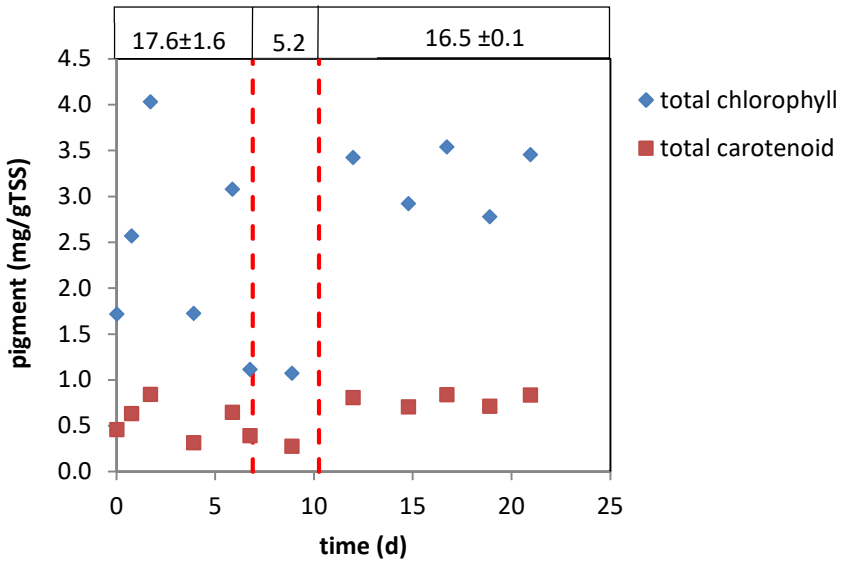

Figure S9: Change in pigment concentration during the mixed green microalgal culture cultivation. Total chlorophyll= chlorophyll a+chlorophyll b. Total carotenoid=violaxanthin+ lutein+ β-carotein.

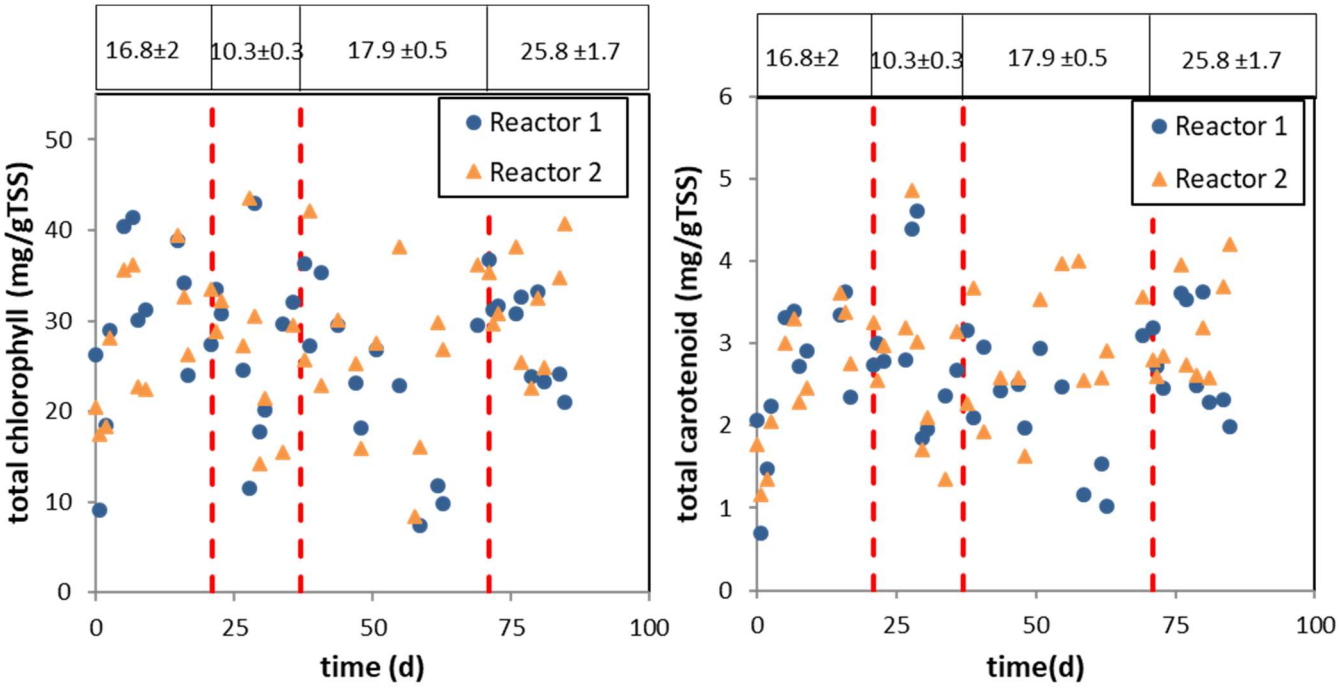

774

775 **Figure S10:** Change in pigment concentration during the *Chlorella sp*. culture cultivation in the reference
776 reactor (Reactor 1) and the reactor where NPR was varied (Reactor 2). Total chlorophyll= chlorophyll
777 a+chlorophyll b. Total carotenoid=violaxanthin+ lutein+ β-carotein.

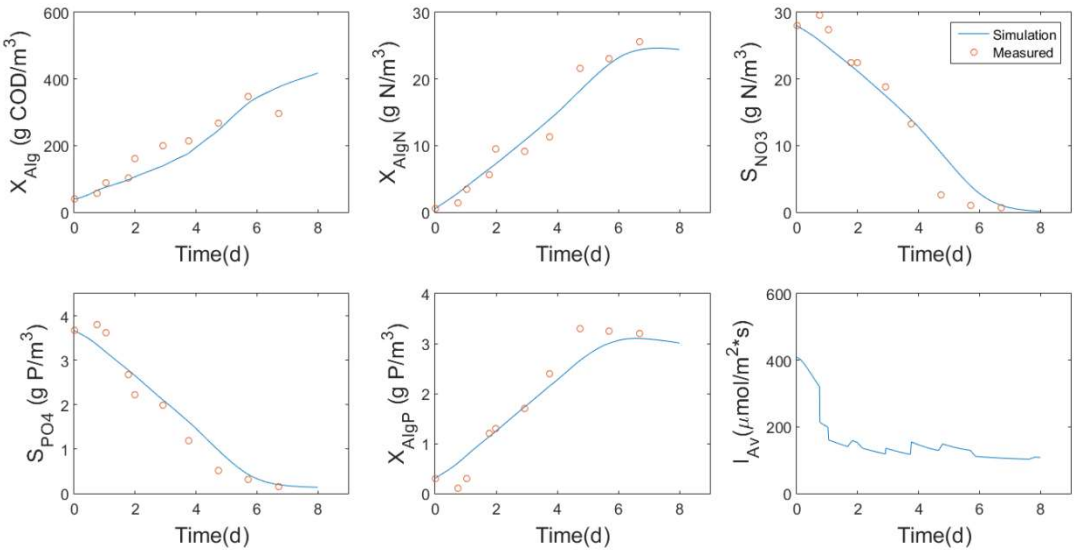

778

779 **Figure S11:** Calibration of the batch where the inoculum was taken after the 10 NPR cultivation and the initial
780 NPR was 17.

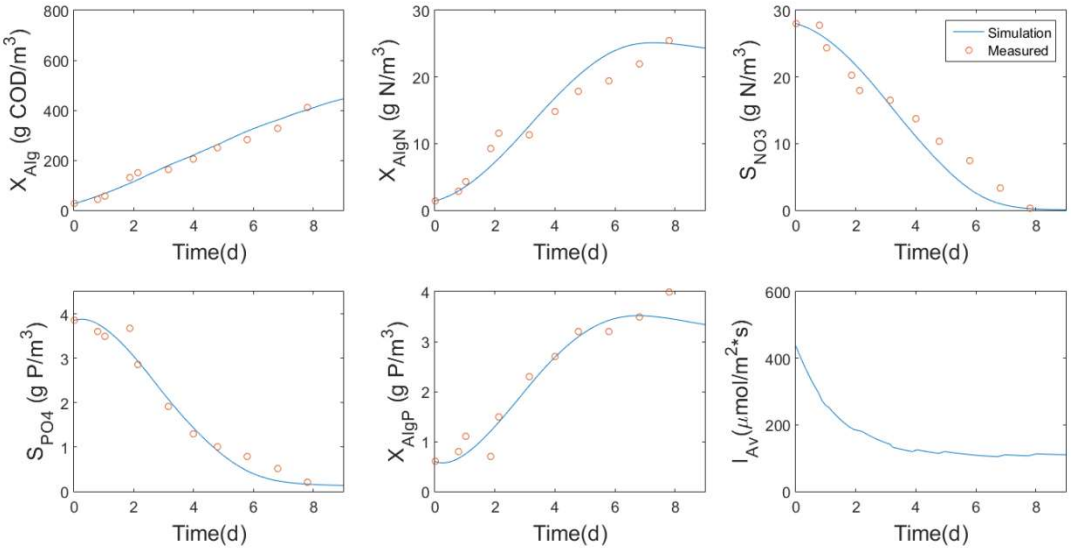

781

782 **Figure S12:** Calibration of the batch where the inoculum was taken after the 25 NPR cultivation and the initial

783 NPR was 17.

784

785

The operation of the laboratory-scale continuous EBPR system

A laboratory scale EBPR system was used to treat domestic wastewater (Fig. S2). It consisted of a sequence of two anaerobic reactors, one aerobic reactor and one clarifier. On Fig. S2 there is a clarifier placed between the anaerobic and aerobic reactors (which can be used for EBP2R operation), however the retention time in this clarifier during the experiments was close to 0. The layout of the plant is shown in Fig. S13.

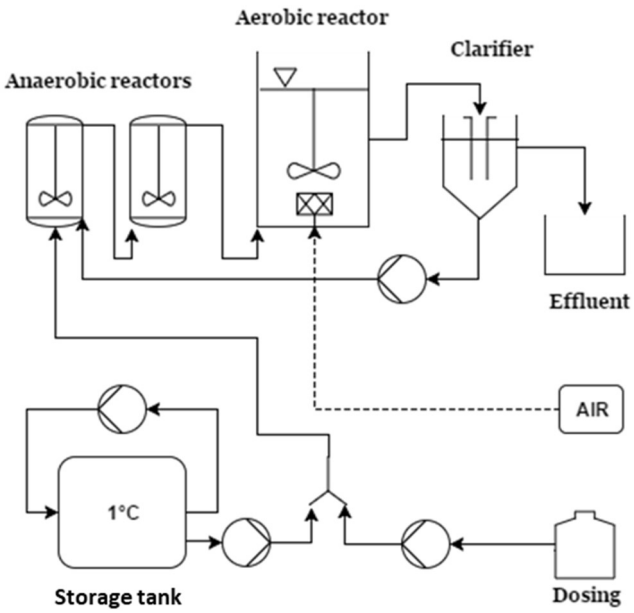

Figure S13: The layout of the continuous EBPR system.

The anaerobic phase was divided into two identical reactors, connected in series, with a working volume of 1.25 L of each reactor. A rotational stirrer working at 60 rpm provided mixing. The aerobic phase consisted of a 5.8 L glass cylinder. Air was provided from the bottom of the reactor by an air diffuser and a rotational stirrer working at 85 rpm provided mixing. A 2 L glass reactor served as the secondary clarifier including a cylinder part and a hopper in the bottom. The system was fed with primary treated domestic wastewater from Mølleåværket WWTP (Kgs. Lyngby, Denmark). The wastewater was stored twice per week in a cooled storage tank, working at 4°C with 180L of working volume, equipped by mixing and internal recirculation. The influent to the EBPR system was obtained by mixing the wastewater with a synthetic solution (rich in sodium propionate), in order to keep the quality of the influent stable in terms of COD and nutrients (N and P). The average values of the final mixture of influent water to the EBPR system were: 36 mg NH_4-N/L, 9.5 mg PO_4-P/L and 430 mg COD/L. The HRT in the system was kept at 13.8 h with an inflow of 11.1 L/day. Recirculation of

807 sludge from the clarifier to the first anaerobic reactor was provided. Moreover, part of the sludge was
808 daily discharged from the aerobic reactor, thus keeping total SRT at 16 days.

809 **Calculation of conversion factor between TSS and COD**

810 Total COD and soluble COD were determined on unfiltered and filtered (0.2 µm membrane filter)
811 samples respectively, using COD test kit (Hach Lange) with a range of 15 – 150 mgO_2/L for filtered
812 samples and with a range of 100-2000 mgO_2/L for unfiltered samples. The COD of the biomass was
813 calculated as the difference between the unfiltered and filtered sample and conversion factor based
814 on the measured TSS was calculated.

815

816

817